Research Article

Luis Suárez*, Mateusz Barczewski, Mark Billham, Andrzej Miklaszewski, Patryk Mietliński, and Zaida Ortega*

Recycling of HDPE-giant reed composites: Processability and performance

https://doi.org/10.1515/gps-2024-0229
received October 28, 2024; accepted January 30, 2025

Abstract: Giant reed (*Arundo donax*), a plant species with potential for obtaining lignocellulosic fibres, was validated as reinforcement in thermoplastic composites with good processability, thermo-mechanical performance, and aesthetics. This study evaluates the impact of closed-loop recycling of high-density polyethylene (HDPE)-based composites with up to 40% of reed fillers: fibres and shredded plants, on their processing and application properties. *Arundo* fillers do not significantly impact the processing stability and performance of recycled composites and can improve some aspects. Minor chemical composition differences were observed, highlighting oxidation resistance. All formulations keep their viscous character and reduce the melt flow index slightly, benefiting reprocessing due to the absence of degradation-prone coupling agents. The composites remain thermally stable up to 230°C, with only slight weight loss at 160°C due to lignocellulosic filler degradation. Fillers lead to longer oxidation induction time compared to neat HDPE. Reprocessed moulded materials show higher stiffness and improved ultimate tensile and flexural strength, but lower impact resistance due to shorter filler length. Smaller fillers and improved matrix distribution also reduce water uptake. Fibrous fillers reduce the aspect ratio, making composites with shredded reed more similar to reed fibres, which are costlier to produce. Shortening of the reprocessed fibrous filler is associated with increased crystallinity in composite materials.

Keywords: giant reed, natural fibres, composites, recycling, reprocessing

*** Corresponding author: Luis Suárez,** Departamento de Ingeniería Mecánica, Universidad de Las Palmas de Gran Canaria, Edificio de Ingenierías, Campus universitario de Tafira Baja, 35017, Las Palmas, Spain, e-mail: luis.suarez@ulpgc.es
*** Corresponding author: Zaida Ortega,** Departamento de Ingeniería de Procesos, Universidad de Las Palmas de Gran Canaria, Edificio de Ingenierías, Campus universitario de Tafira Baja, 35017, Las Palmas, Spain, e-mail: zaida.ortega@ulpgc.es
Mateusz Barczewski: Poznan University of Technology, Institute of Mechanical Technology, Piotrowo 3, 61-138, Poznań, Poland
Mark Billham: AMIC-PPRC, Queen's University of Belfast, Ashby Building, BT9 5AH, Belfast, Northern Ireland, United Kingdom
Andrzej Miklaszewski: Poznan University of Technology, Institute of Materials Science and Engineering, Jana Pawla II 24, 61-139, Poznan, Poland
Patryk Mietliński: Poznan University of Technology, Institute of Mechanical Technology, Division of Metrology and Measurement Systems, Piotrowo 3, 61-138, Poznan, Poland

1 Introduction

Increased global awareness of using sustainable resources to reduce the carbon footprint of the manufacturing industry has driven the search for new bio-based materials. Recycling and reuse strategies have also promoted advances in the recovery and upcycling of these materials. In the field of polymers and composites processing, besides the development of novel materials formulated from renewable sources and the move away from overexploitation of fossil resources, the introduction of natural fibres, such as the lignocellulosic ones, has also reduced the amount of plastic in various applications. The use of natural fibres for composite production not only allows a reduction in the consumption of polymeric matrices but also promotes the development of advanced materials with improved attributes such as better specific properties, thermal or acoustic insulation, and low cost [1,2]. Moreover, fillers derived from plant resources, besides promoting the biodegradation of polymeric compounds [3,4], represent a great opportunity for the development of more sustainable recycling strategies compared to those based on fillers of synthetic origin, such as glass or carbon fibres [5].

Giant reed (*Arundo donax* L.) is a versatile plant species that has attracted great interest due to its potential applications in green biorefineries and sustainable materials. Its high biomass yield, adaptability to different environments and low cultivation requirements make it an attractive candidate for the production of biofuels, biochemicals, and other value-added products [6,7]. This plant

species, native to East Asia and widespread in subtropical and warm temperate climates around the world, can be used to produce biofuels such as biogas and bio-ethanol through biological fermentation, as well as bioenergy through direct biomass combustion [8,9]. Its high biomass production and low input requirements make it a competitive energy crop compared to other lignocellulosic feedstock [10,11]. The plant can be processed to obtain various high-value compounds, including levulinic acid, oligosaccharides, fermentable sugars, and polyphenols, demonstrating its potential for green chemistry applications [6,12]. Its biomass can also be used for producing wooden building materials such as bricks or particleboards, enhancing its role in sustainable construction [7,13–15]. In addition, its role in phytoremediation and environmental management further underscores its potential in advancing sustainable development goals. Giant reed is capable of growing in contaminated soils and improving soil fertility by accumulating pollutants in its biomass [16,17] and can be used to remove pollutants from wastewater [18], thereby improving water quality and contributing to environmental sustainability.

On the other hand, polyolefins, a class of polymers derived from olefinic hydrocarbons, or alkenes, whose discovery dates back to the 1930s, have grown exponentially since then and revolutionized the global plastics industry. These materials have transformed modern life and are still the subject of intense research and development because of their diverse applications. Due to their versatility, low cost, and mechanical properties, polyolefins have consolidated their position as the most widely manufactured and used plastic worldwide. This family of thermoplastics, including polyethylene (PE) and polypropylene (PP), make up the majority of the global plastics market, with their use and production continually increasing, reaching the global output of nearly 220 million tons/year [19]. In fact, polyolefins accounted for almost half of the demand from plastic converters in Europe in 2021 [20]. Its use in a variety of applications, including food packaging, industrial products, consumer goods, structural plastics, and medical applications, has made its recyclability a critical issue, primarily due to its extensive use in short-term applications such as packaging [21]. PE, in particular, leads the plastics industry with a market share of over 31% [4] and stands out for its versatility to be used as a matrix in the production of composites due to its excellent properties and wide range of applications. Characteristics such as toughness, near-zero moisture absorption, chemical inertness, low coefficient of friction, ease of processing, and unique electrical properties make it an ideal candidate for use in composite materials, where it can serve as a robust matrix that enhances the overall performance of the composite [22]. Moreover, PE is not only the most commonly used thermoplastic in the polymers and composites industry but also offers great potential for continuous closed-loop recycling. Research has shown that high-density polyethylene (HDPE) can be reprocessed several times while maintaining compatible performance characteristics, thus mitigating the impacts of plastic waste [23,24].

The addition of a large variety of plant-based fillers such as jute [25], hemp [26], sugarcane bagasse [27], spent coffee grounds [28], peanut shells [29], palm [30], banana [31], or sisal fibres [32] into an HDPE matrix has been widely studied as a way to produce more sustainable materials. This strategy of obtaining biocomposites usually improves the mechanical properties of HDPE, including significant increases in stiffness and elasticity and reduces thermal stability. Good interfacial adhesion between fibres and the HDPE matrix is crucial for enhancing mechanical performance. Treatments such as mercerization, chemical functionalization, and the use of compatibilizers like maleic anhydride grafted PE have been studied [33]. However, there is still a gap in the study of the recyclability of these materials, the literature found on the effects of their reprocessing remains limited [34,35]. Not surprisingly, the properties of recycled polyolefin-based natural fibre composites (NFCs), including their viscosity, average molecular mass, crystallinity, and fibre dimensions, are significantly affected by thermo-mechanical reprocessing. Minimizing thermal degradation, oxidation, aesthetics, or mechanical performance deterioration of such materials requires careful consideration of various recycling parameters, including screw rotational speed, throughput rate, and barrel temperature profile among others [36].

In the previous work, giant reed has proven to be a promising plant species for obtaining high value-added fibres [37]. Its potential application as a reinforcing material in PE-based composites has also been reported [38,39]. These composites have excellent thermal stability allowing a wide processing window, interesting mechanical performance with efficient stress transfer and good aesthetics. The present work explores these materials in depth to analyze the effects of thermo-mechanical closed-loop recycling and to determine the changes in processability and in-use performance parameters upon reprocessing.

2 Materials and methods

2.1 Materials

NFC, based on a HDPE matrix and lignocellulosic fillers from giant reed (*Arundo donax* L.), were prepared by

twin-screw extrusion compounding, as described in a previous work [38]. The polymer used was HDPE grade HD6081 from Total Petrochemicals, with a melt flow index (MFI) of 8 g/10 min (190°C/2.16 kg) and a density of 960 kg·m^{-3}, according to the producer's specifications. Besides, two different forms of Arundo-derived materials were used as reinforcement phase of the composites, namely, fibres (F), extracted from the stems of giant reeds, and shredded material (S), obtained by grinding aerial parts (stems and leaves) of the same plant species. Reed fibres were obtained after 1 week of soaking in an alkaline solution and further processing using a roller press. Once the fibre bundles were extracted from the stems, they were washed in water to neutral pH, dried, cut to a length of 3–5 mm, and sieved to remove fines and clustered particles. The procedure for preparing the shredded material consisted of chopping and drying the collected plants, shredding them with a laboratory rotary mill, washing the shredded material, drying, and sieving [37]. The fibres were cut to approximately 3 mm length, showing a diameter of 157 ± 74 μm, while shredded material shows an average particle size of 370 ± 133 μm [37,40,41]; fibre length is reduced to 781 ± 288 μm after compounding obtaining [38,40,42].

The composite materials were named according to the type and amount of lignocellulosic filler (in% by weight): PE.F20 and PE.F40 correspond to composites with 20% and 40% Arundo fibres respectively, while PE.S20 and PE.S40 refer to composites produced with 20% and 40% Arundo shredded material. Before recycling, the physicochemical, rheological, and thermomechanical properties of the compounds, produced by the ThermoScientific Process11 twin-screw extruder with temperatures from 170°C to 185°C, with the profile shown in the previous work [38], and the test specimens, subsequently moulded by an Arburg 320S injection moulding machine, were determined [38].

2.2 Recycling process

The original moulded parts (cycle 0) were ground at 1,400 rpm in an Alpine Augsburg shredder machine (model RO 16/8) and then reprocessed up to five times (cycles 1 to 5) using a ThermoScientific Haake Rheomex PTW 16 OS twin-screw extruder to evaluate the effect of mechanical recycling on performance of the HDPE-Arundo composites. Reprocessing was performed with a screw rotation speed of 300 rpm and the following hopper-to-nozzle temperature profile: 170-175-170-165-165-160-160°C. The used extruder has an L/D ratio of 25 and a screw profile with three kneading zones as shown in Figure 1.

The same process was repeated separately for the four Arundo composite formulations (PE.F20, PE.F40, PE.S20, and PE.S40) as well as for the neat HDPE polymer (PE). After completing the five thermo-mechanical reprocessing cycles, the materials were remoulded again using an Arburg 320S injection-moulding machine (cycle 6). The nomenclature used to designate materials after this reprocessing step includes the suffix -r at the end of the name of each formulation, thus PE-r, PE.F20-r, PE.F40-r, etc.

The manufacturing parameters used for injection moulding were as follows: temperature profile (from hopper to nozzle) set at 175-180-185-185-190°C, mould temperature at 30°C, cooling time of 15 s, back pressure of 5 MPa, holding pressure of 50 MPa, and dosing volume of 50 cm3. Switchover pressure was recorded for each moulding and averaged for the different composites. Materials were dried at 60°C (−40°C dew point) overnight before processing.

2.3 Characterization

The recycled materials were subjected to several characterization tests, both on pellets and injection-moulded specimens. Prior to the moulding process, the compounds were analyzed chemically, thermally, and rheologically using Fourier transform infrared (FTIR) spectroscopy, thermogravimetry (TGA), differential scanning calorimetry (DSC), MFI, and oscillatory and capillary rheometry. In addition, the effects of the recycling process on the morphology (length, diameter, and aspect ratio) of the reinforcing particles as well as on the density and porosity of the composite materials were assessed using microcomputed tomography and optical microscopy. The injection-moulded samples were also evaluated for a number of other attributes, including hygroscopicity, changes in appearance (colour and gloss), wide-angle

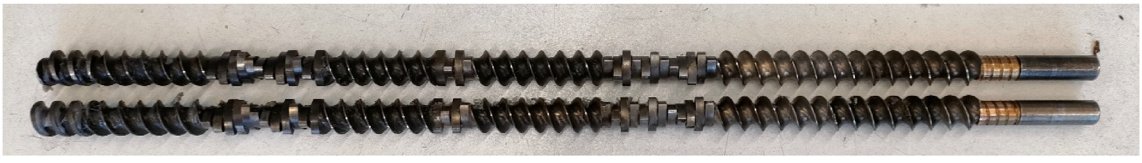

Figure 1: Screw profile configuration.

X-ray scattering (WAXS), mechanical behaviour (hardness, tensile, flexural, and impact strength), dynamic mechanical thermal analysis (DMTA), heat deflection temperature (HDT), Vicat softening temperature (VST), thermal diffusivity, and thermal expansion.

FTIR spectra were obtained using a Spectrum 100 spectrophotometer from Perkin Elmer, under attenuated total reflectance mode with a zinc selenide single bounce crystal. Each spectrum was recorded with 64 scans at a resolution of 4 cm^{-1}, covering wavelengths between 4,000 and 600 cm^{-1}.

Rheological behaviour was assessed using both oscillatory and capillary rheometry. For realization tests in the oscillatory mode, the AR G2 rheometer from TA Instruments, with parallel plates of 25 mm diameter, was used. The oscillatory tests were conducted in a nitrogen environment at 190°C, and with a 2.5 mm gap. The strain sweep mode was used for preliminary testing so that subsequent experiments take place in the linear viscoelastic (LVE) region. The range of strain in these tests was 0.1–5%. In the LVE region, angular frequency sweeps between 0.01 and 100 rad·s^{-1} were carried out at 0.5% strain. Dynisco LCR 7000 rheometer was used for capillary tests. A capillary die of 2 mm diameter (D) and L/D = 20 was applied. The presented results were subjected to the Rabinowitsch correction, while the Bagley correction was omitted due to the use of a die with a high L/D ratio. The applied temperature for the capillary test was 190°C. Furthermore, MFI of each material was determined according to ISO 1133 on a Kayeness Inc. 7053 apparatus (Dynisco Company) using a load of 2.16 kg and a temperature of 190°C.

The thermal properties of the materials were obtained by DSC and thermogravimetric analysis using a Perkin Elmer DSC 4000 apparatus and a Perkin Elmer TGA 4000 device, respectively. Nominal samples of 10 ± 0.2 mg were prepared using sealed aluminium crucibles under a nitrogen atmosphere for DSC analysis. Thermogravimetric experiments were performed between 30°C and 900°C by heating the samples at 10°C·min^{-1} in open alumina crucibles, while DSC measurements were performed from 30°C to 200°C at the same heating rate and with two heating cycles. Melting temperatures were determined for both cycles (T_{m1} and T_{m2}, respectively) and crystallization temperatures (T_c) for the cooling step. Finally, the enthalpies of melting and crystallization (H_{m1}, H_{m2}, and H_c) were also calculated and used to obtain the degree of crystallinity (χ), as from Eq. 1:

$$\chi = \frac{1}{1 - m_f} \cdot \frac{\Delta H_m}{\Delta H_0} \cdot 100 \quad (1)$$

DSC was also applied to determine the oxidation induction time (OIT) according to the standard ISO 11357-6. For this purpose, the samples were heated from 30°C to 220°C (heating rate 20°C·min^{-1}) under nitrogen flow and then kept at 220°C for 5 min in nitrogen; the gas was then switched to oxygen, and the time required for sample oxidation was measured.

WAXS tests were carried out with Pan-analytical Empyrean, Almelo (Netherlands) equipment with the copper anode (Cu-Kα – 1.54 Å, 45 kV, and 40 mA) in the Bragg–Brentano reflection mode configuration. The measurement parameters were adjusted to 3–60° 2 theta, with a 45 s per step 0.05°. Applying the deconvolution procedure using the Lorentzian function allows the separation of the amorphous and crystalline components from the obtained diffraction patterns. The crystallinity has been calculated according to Eq. 2 [43]:

$$X_{WAXD} = \frac{A_{cr}}{A_{cr} + A_{am}} \cdot 100\% \quad (2)$$

where A_{cr} is the sum of the area of scattering from the crystalline phase and A_{am} is the sum of the area of amorphous scattering of tested PE-based samples.

For injection-moulded specimens, HDT was determined according to ISO 75 (heating rate of 120°C·h^{-1} and load of 1.8 MPa). The VST was measured at a load of 50 N and a heating rate of 50°C·h^{-1} according to ISO 306 B50. The TPC/3 TOP VST/HDT device was used for both tests, with a minimum of three measurements for each series to average the results.

A modified Ångström method was used with a Maximus instrument (Poznan, Poland) to analyze the thermal diffusivity, following a procedure outlined by [44]. The samples were heated at 400 s using a 23 V charge on the microheater during the experiment. Thermal diffusivity (D) is determined by Eq. 3, which involves thermal conductivity (λ), density (ρ), and specific heat capacity at constant pressure (c_p) [45].

$$D = \frac{\lambda}{c_p \cdot \rho} \quad (3)$$

Thermal expansion tests were conducted using the Netzsch Hyperion TMA 402 F1 device, heating at 2°C·min^{-1} with 100 mL·min^{-1} argon flow. Measurements covered −100°C to 100°C, split into −100°C to 25°C and 25°C to 100°C, applying 0.01 N force. Analysis was done with Netzsch Proteus software.

The variation in filler morphology was assessed before and after recycling of the composites using the method described in a previous publication [40]. Images were taken with a high-resolution flatbed scanner, Canon CanoScan LiDE 400, at 4,800 dpi and analyzed with ImageJ software to determine the length, diameter, and aspect ratio of the lignocellulosic fibres and particles.

The impact of recycling on the filler distribution and porosity of the injection-moulded samples were evaluated

using X-ray tomography, model v|tome|x s240 (Waygate Technologies/GE Sensing & Inspection Technologies GmbH), with the following specific settings: 150 kV voltage and 200 µA current for the Microfocus X-ray tube, 150 ms exposure time per image, and 123 µm voxel size.

The density of the materials was measured according to ISO 1183 using Archimedes' principle. This was done using a methanol medium at room temperature on a Sartorius AG precision balance. Each sample was subjected to five measurements to obtain a mean value and standard deviation.

The water absorption test, as per ISO 62, involved soaking the samples in deionized water at 23°C and measuring their weight until a stable mass was achieved. The water absorption (W) was calculated using Eq. 4 on three replicas of each sample.

$$W(\%) = \frac{W_t - W_0}{W_0} \cdot 100 \tag{4}$$

Fick's law was used to determine the rate at which water is absorbed, also calculating the diffusion coefficient:

$$D = \pi \cdot \left(\frac{k \cdot h}{4 \cdot W_m}\right)^2 \tag{5}$$

In the aforementioned formula, D represents the diffusion coefficient, h is the original sample thickness, W_m is the maximum moisture absorbed, and k is the initial slope of the water uptake curve versus $t^{1/2}$:

$$k = \frac{W_1 - W_2}{\sqrt{t_2} - \sqrt{t_1}} \tag{6}$$

Tensile and flexural tests were carried out using a Lloyd LS5 universal testing machine according to ISO 527 and ISO 178 standards, with five replicas for each material and test type. In both cases, the tests were done at a strain rate of 2 mm·min^{-1} to determine the elastic moduli and 10 mm·min^{-1} to evaluate the ultimate strengths. Impact strength was measured on notched specimens using a Ceast Resil impact machine in Charpy mode per ISO 179–1/1eA:2023, with a 7.5 J pendulum, 62 mm span, and 3.7 m·s^{-1} impact speed, with 10 specimens tested. Ball indentation hardness was measured according to the ISO 2039 standard using a KB Prüftechnik device, with at least seven measurements per material series and a load of 132 N. Average values and standard deviation are provided for all properties.

DMTA was used to assess the thermo-mechanical properties of each material using a Tritec 2000 device (Triton Technology). The evaluation was conducted under the single cantilever bending method, applying a strain of 10 µm at 1 Hz frequency and a heating rate of 2°C·min^{-1} over the temperature range of −100°C to 100°C. From the DMTA results, the brittleness (B) and the adhesion factor (A) of the different materials by using Eqs. 7 and 8 as proposed by Brostow et al. [46] and Kubát et al. [47], respectively, were calculated.

$$B = \frac{1}{\varepsilon_b \cdot E'} \tag{7}$$

where ε_b is the elongation at break and E' is the storage modulus, both at room temperature.

$$A = \frac{1}{1 - x_F} \cdot \frac{\tan\ \delta_C}{\tan\ \delta_{PE}} - 1 \tag{8}$$

In Eq. 8, χ_F is the volume proportion of the filler in the composite, and tan δ_C and tan δ_{PE} are the damping factors of the composite and the matrix.

The entanglement factor (N) and reinforcement efficiency (r) were also assessed to measure the strength of the filler–matrix interaction. The entanglement factor (N) is calculated as follows:

$$N = \frac{E'}{R \cdot T} \tag{9}$$

In this case, R is the universal gas constant and E' is the storage modulus at a specific temperature (T), in Kelvin.

Finally, the reinforcement efficiency (r) is determined from the ratio between the storage modulus of the composite (E'_c) and the matrix (E'_m), taking into account the volume fraction of the filler (V_f):

$$E'_c = E'_m\ (1 + r \cdot V_f) \tag{10}$$

Changes in the aesthetic appearance of the materials after reprocessing were evaluated by optical spectroscopy, using a HunterLab Miniscan MS/S-4000S spectrophotometer for colour measurement ($L^*a^*b^*$ coordinates), and a Test An DT 268 glossmeter for determination of gloss according to ISO 2813 at measuring angles of 20°, 60°, and 85°. The total colour difference parameter (ΔE^*) is determined as shown in Eq. 11:

$$\Delta E^* = [(\Delta L^*)^2 + (\Delta a^*)^2 + (\Delta b^*)^2]^{0.5} \tag{11}$$

3 Results and discussion

3.1 Chemical structure and composition

Reprocessing of polyolefins and polyolefin-based composites is associated with the formation of various functional groups that indicate oxidative degradation. FTIR analysis has revealed increases in absorption bands corresponding to carboxylic acids, ketones, aldehydes, alcohols, and

ethers. These peaks suggest ongoing oxidation and breakdown of the polymer matrix and reinforcing fibres, particularly evident after multiple cycles [36,48]. The intensity and presence of specific peaks in the spectra can change substantially after several reprocessing cycles. For instance, the increase in absorption bands associated with oxidative degradation can show more significant oxidation levels in composites with repeated processing. Such oxidation profiles can be quantified by measuring peak heights and areas as indicators of degradation [49].

Figure 2 shows the changes observed in the FTIR spectra for the original and recycled materials. The peak patterns are very similar, with only minor variations among the different formulations of composites, both before and after recycling. Comparable results were reported by Bhattacharjee and Bajwa after six recycling cycles on HDPE composites filled with 30% wood flour [50] and by Fonseca-Valero *et al.* for five-cycle reprocessed HDPE-matrix composites with 48 wt% of cellulose fibres [49]. The broad band attributed to the O–H groups in the range of 3,600–3,000 cm^{-1}, which was originally more intense in composite materials with 40% lignocellulosic fillers, completely disappears in all formulations after reprocessing. Meanwhile, the C–H peaks characteristic of HDPE-based composites, wavenumbers around 2,920, 2,850, 1,470, and 720 cm^{-1}, are still present even after the reprocessing cycles. This is consistent with the literature, where several studies have demonstrated the oxidation resistance of HDPE [23].

On the other hand, the vibration band peak in the double bond region (above 1,500 cm^{-1}) also disappears after recycling. The same trend is observed for the peaks in the fingerprint region from 1,400 to 750 cm^{-1}. The high-intensity peak at 1,016 cm^{-1}, which shows the C–O group of cellulose in the original composites, does not completely disappear, but its signal is greatly attenuated after reprocessing.

This flattening of fingerprint characteristic absorption bands originating from the lignocellulosic filler may be related to a more homogeneous composite structure. Macromolecules of polyolefins subjected to multiple processing are shortened, which causes a decrease in the polymer viscosity [51]. The proposed analysis method is based on measurements performed for the injected surface of the samples. Due to the shortening of the fibre length and changes in the rheological properties, the surface of the injection moulded reprocessed sample reveals a homogeneous polymer skin layer without filler inclusions. It should be emphasized, however, that in the case of none of the analyzed samples, the appearance of additional absorption bands was noted in the range of the formation of carbonyl groups (1,600–1,800 cm^{-1}), thus meaning that no changes related to intensive degradation changes of PE matrix have aroused [52].

3.2 Rheological behaviour

3.2.1 MFI

From a rheological perspective, the processing stability of thermoplastic compounds can be assessed by examining changes in MFI [24] and, consequently, by observing fluctuations in V/P switchover pressure (changeover from the velocity to pressure control) during injection moulding [53]. The MFI of polymers tends to increase with recycling, indicating changes in molecular weight and flow behaviour. This increase may be attributed to chain scissions,

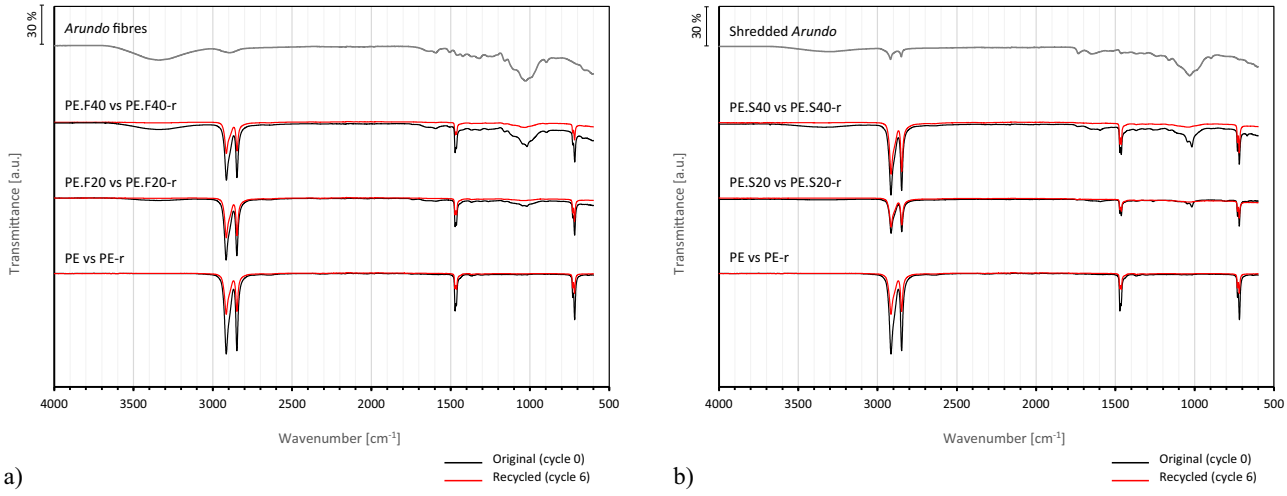

Figure 2: FTIR spectra of original (cycle 0) versus recycled composite (cycle 6) with (a) fibre and (b) shredded fillers.

in which polymer chains are broken down into shorter lengths, which can lead to increased susceptibility to oxidation. From the injection moulding side, it is worth highlighting that a steady feed in the plasticizing process is necessary to ensure product quality in terms of homogeneity, operational stability, and production speed. While continuous reprocessing of high- or low-density PE results in more difficult injection moulding due to a progressive decrease in MFI [54], the incorporation of *Arundo* fillers into the thermoplastic matrix not only does not increase the difficulty of processing but also seems to make it somewhat easier. Thus, after the reprocessing cycles, all material series show a slightly higher MFI, which is more noticeable in the biocomposites with shredded reed filler, as shown in Figure 3. Similar behaviour was observed by Fonseca-Valero et al. [49], which they attributed to the cellulose fibre degrading as a result of shear stresses, compression, and elongation on the melt during reprocessing. The size reduction of the lignocellulosic fillers, which was confirmed by microscopic observation and measurement, as described later, contributed to this behaviour.

Therefore, when comparing pure HDPE with PE.F40-r series, the required moulding pressure is only about 40% higher after recycling due to an increase in the melt flow rate and homogenization of the material blend. Any composite formulation resembles the behaviour of the PE matrix in this respect and shows no noticeable signs of deterioration.

Several studies on natural fibre-reinforced polyolefin composites have found an increase in viscosity as a result of chemical treatments to improve the matrix-reinforcement interface [55]; also lubrication effects produced by coupling agents have been reported [56]. However, it has also been concluded that these effects largely disappear with recycling cycles [57]. The lack of binding additives or treatments in the HDPE-*Arundo* compounding favoured a slight improvement rather than a worsening of processability throughout the closed-loop recycling.

3.2.2 Oscillatory and capillary rheometry

The rheological properties, which directly influence the moulding process, are assessed by rheological curves obtained by oscillatory (Figure 4) and capillary rheometry (Figure 5).

Different behaviours were observed depending on the geometry of the measuring system, which resulted from the characteristic flow properties of filled polymeric systems. From oscillatory rheology tests, it can be seen that fibrous composites tend to increase viscosity, while composites with shredded material show a lower impact on complex viscosity, which can be related to the lower ability of this filler to create a 3D physical network of hindered particles in composite melt compared to fibres. In all samples, a predominant viscous character is evidenced by a higher loss moduli compared to storage one. Fibrous composites tend to increase the storage modulus with reprocessing along the angular frequency analyzed, while the series with shredded materials show the opposite behaviour. In any case, the differences between the curves before and after recycling decrease with increasing filler and are lower for fibrous composites than shredded plant material. Finally, no significant changes in the rheological behaviour of the pure PE were observed, supporting the

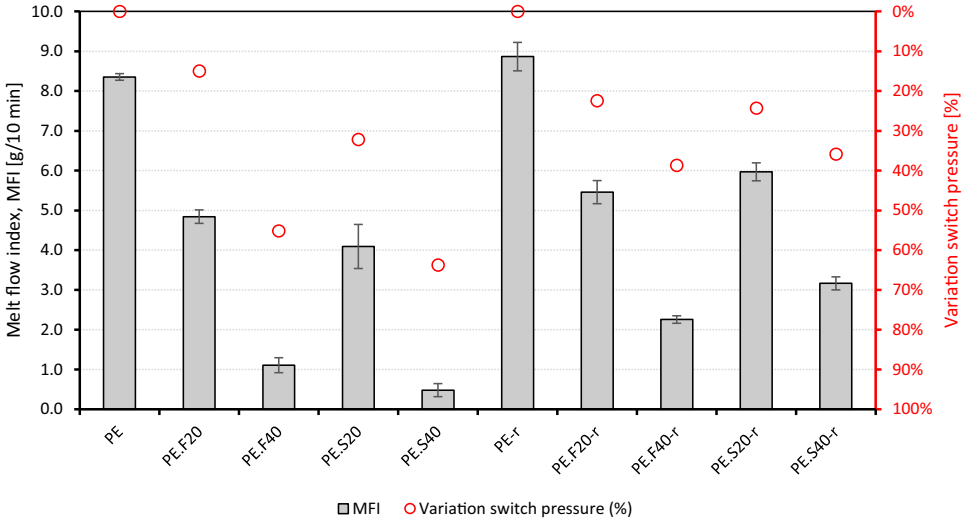

Figure 3: MFI and switchover pressure variation for the different materials.

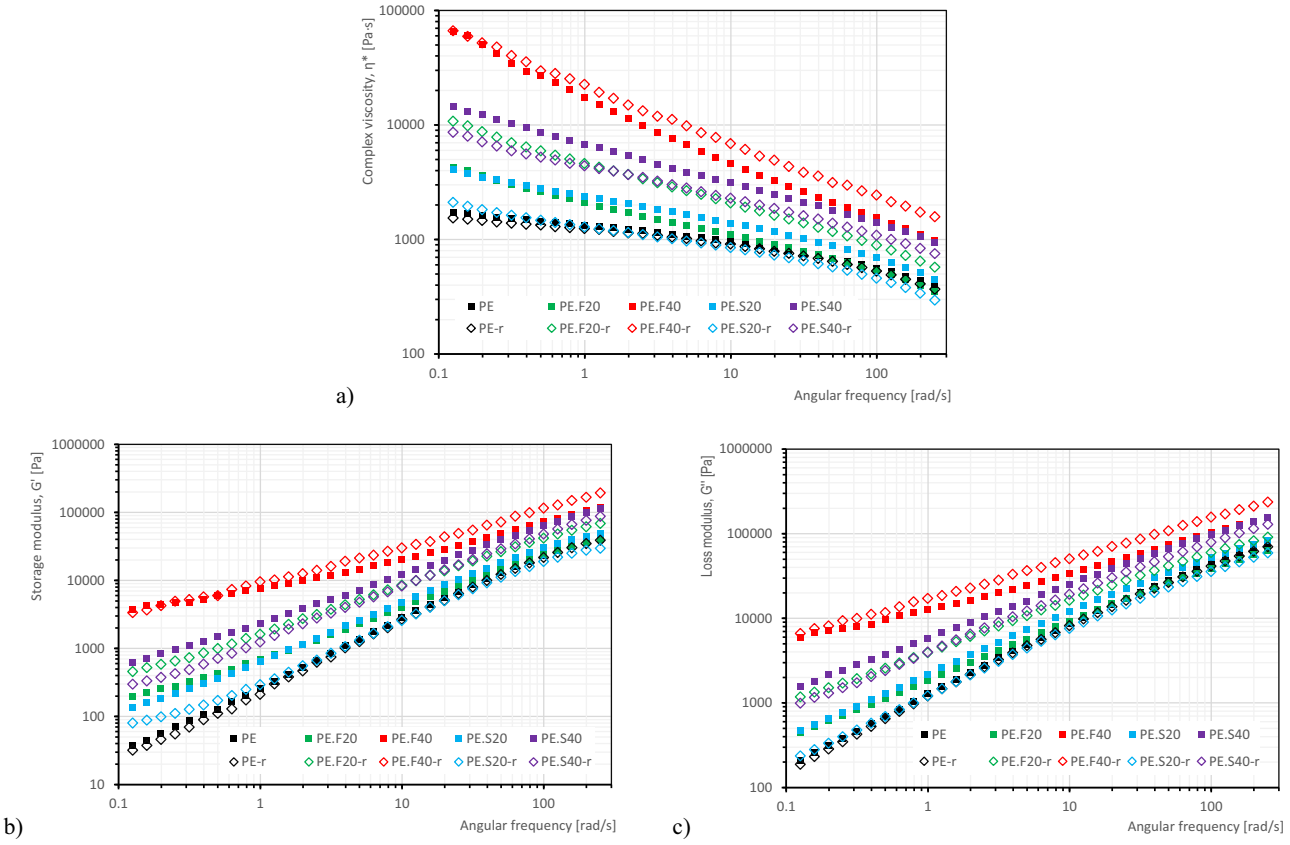

Figure 4: Oscillatory rheology results: (a) complex viscosity, (b) storage modulus, and (c) loss modulus.

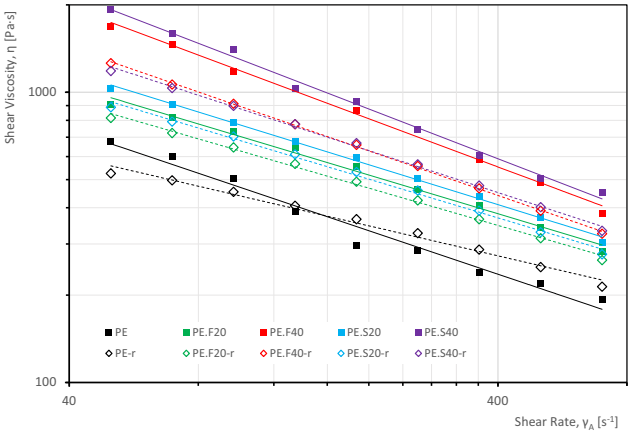

Figure 5: Capillary rheology results: Shear viscosity vs shear rate.

FTIR observations by showing that the matrix does not undergo oxidation or cross-linking as a result of reprocessing.

In addition, from capillary rheology tests (Figure 5), it was found that both before and after reprocessing, the fibrous composite materials were characterized by slightly lower viscosities compared to the shredded ones. This may be because the fibres can align more easily in the direction of flow [58,59]. Finally, the flow resistance of the composites with 40% filler after recycling is almost identical regardless of the type of filler.

3.3 Thermal behaviour

3.3.1 TGA

The thermogravimetric analysis (Figure 6) shows that all compounds remain thermally stable, even after recycling, up to approximately 40°C above the processing temperature, despite a small weight loss (lower than 2%) upon reaching 160°C, which is only noticeable in the 40% loaded composites, and probably due to an initial degradation of the lignocellulosic fillers after multiple reprocessing. Similarly to the original composites, the thermal stability of the recycled compounds varies depending on the loading percentage, regardless of the type of filler, with the first degradation peak (from derivative thermogravimetry [DTG]) occurring around 350°C. The PE.F40-r and PE.S40-r formulations undergo a faster degradation, resulting in a mass loss of around 25% at this initial peak, related to the biomass degradation; however, the composites with 20%

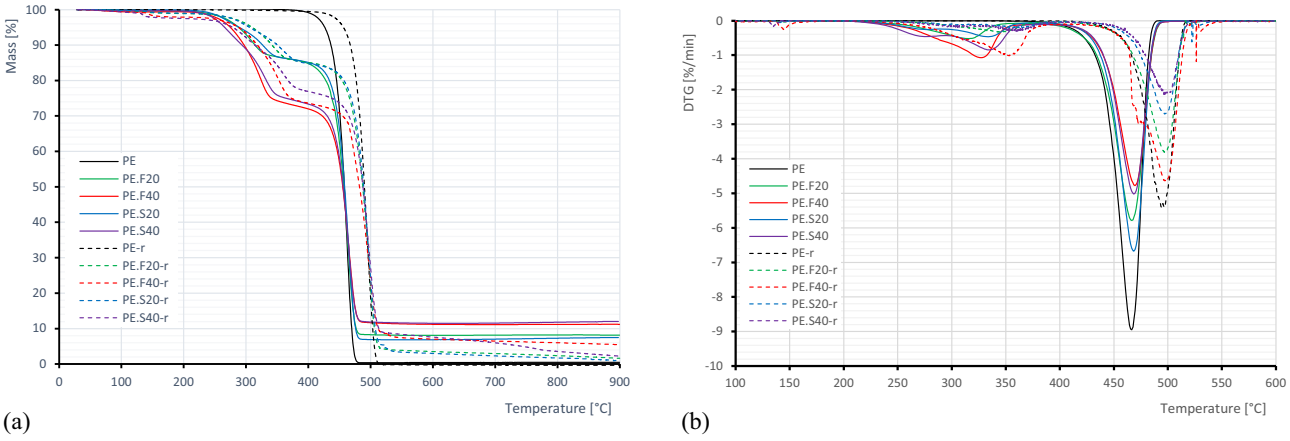

(a) (b)

Figure 6: (a) TG and (b) DTG curves pre- and post-recycling processes.

lignocellulosic material degrade at a much slower rate; this is following the same trend observed in the nonrecycled materials. Thus, the increase in the amount of plant filler correlates with a higher weight loss due to thermal degradation of said filler, as expected. In any case, the most significant peak occurs when the decomposition temperature of the HDPE matrix is reached. After the recycling cycles, this point is delayed by about 30°C for all materials due to the removal of volatile or labile compounds during the previous processing [50,56,60]. Regarding the residual mass after reaching 900°C, also the composite with 40% fibres is the only one in which the amount of inorganic compounds present after carbonization exceeds 5% of the initial mass.

3.3.2 DSC

Based on DSC results, it can be seen that the recycling process minimally affects the temperatures of the phase transitions. When analyzing the thermal behaviour before and after reprocessing, it is noted that there are no major variations in melting temperatures, with T_{m2} in the range of 134.6–135.6°C for all materials, and only a minimal rise in crystallization temperatures, less than 5°C for recycled ones, as shown in Table 1. These findings align with previous research on HDPE-based composites, indicating that neither the presence of lignocellulosic materials nor reprocessing cycles significantly influence melting and crystallization temperatures [61,62].

On the other hand, it has been observed that neat HDPE experiences a decrease in the enthalpies of melting and crystallization after going through reprocessing cycles, whereas the lignocellulosic-filled materials exhibit a noticeable increase of 20–40% in energy flow compared to the original composites. The composite materials also show a slight increase in their degree of crystallinity, which can be attributed to the reduction in particle size and its nucleation effect, as described by Chen and Yan [63]. These authors correlate the nucleation ability of lignocellulosic fibres in HDPE-based composites (without any coupling agent) not only with their topography, surface energy, wettability, and chemical composition but also with the presence of

Table 1: DSC test results for all materials before and after reprocessing

Material	T_{m1} (°C)	T_{m2} (°C)	T_C (°C)	ΔH_{m1} (J·g^{-1})	ΔH_{m2} (J·g^{-1})	ΔH_C (J·g^{-1})	χ_1 (%)	χ_2 (%)	OIT (min)
PE	132.7	135.3	112.9	175.4	172.6	193.3	59.9	58.9	36.8
PE.F20	136.9	134.7	111.5	118.7	125.8	135.8	50.6	53.7	51.3
PE.F40	132.7	133.9	113.1	108.6	109.5	108.4	61.8	62.3	76.1
PE.S20	137.2	136.2	111.1	119.4	128.4	140.8	50.9	54.8	45.4
PE.S40	133.0	135.0	112.1	76.4	79.8	82.5	43.5	45.4	27.1
PE-r	134.6	135.6	116.5	142.7	164.6	165.2	48.7	56.2	7.9
PE.F20-r	135.6	135.5	114.1	156.5	156.4	164.1	66.8	66.7	19.3
PE.F40-r	136.8	135.6	113.5	134.2	152.5	155.2	76.3	86.8	29.4
PE.S20-r	133.9	135.0	114.5	139.3	165.2	172.5	59.4	70.5	18.1
PE.S40-r	136.4	134.6	117.0	101.9	96.6	95.7	58.0	55.0	11.8

fibres of very short length (1.15 ± 0.86 mm), in the same size range used in the present work.

3.3.3 OIT

The reprocessing of polymer composites can have profound effects on their oxidation stability. Thermal processing can cause oxidation of polymers, which can be accelerated by factors such as high processing temperatures and extended residence times in the extruder [64]. Prolonged exposure to high temperatures near decomposition points can result in the formation of decomposition products that further alter material properties. Thus, degradation resulting from repeated exposure can lead to weaker bonds and unsaturated structures, which negatively impact the composites' mechanical properties and thermal stability [50]. During the first processing cycle, the reed fibre increased the oxidation time of the polymeric compounds (Table 1), even duplicating it in the case of 40% loading with respect to neat PE. After recycling, a drastic reduction in OIT was observed for all materials. However, the formulation with a higher *Arundo* fibre content managed to counteract this effect by only 20% compared to the virgin polymer matrix. Therefore, the *Arundo*-derived fillers are providing interesting stabilizing features to the PE matrix, due to their content in phenolic groups, mainly coming from lignin; other researchers have recently proposed the use of postconsumption coffee or tea solids or spent brewery grains as a way to valorize these residues while becoming a source of antioxidant stabilizing the polymer [60,65,66].

3.3.4 Thermal diffusivity

Few studies have been found in the literature on the parameters of thermal diffusivity and how it relates to the dimensional stability of lignocellulosic composites [67]. For some applications, however, it may be very interesting to analyze the heat transfer rate through the material. Figure 7 shows the mean values and standard deviation of the thermal diffusivity of PE and reed composites in injection moulded parts with the original materials and after several thermo-mechanical processing cycles. After the first cycle, only the PE.F40 series showed a significant increase in heat transfer rate, while after reprocessing, all lignocellulosic composites show an increase in their thermal diffusivity.

3.3.5 Thermal expansion

The results of the thermomechanical analysis (TMA) show the changes in length (dL/L_0) and thermal expansion coefficients (α) of the different materials before and after reprocessing, determined in three temperature ranges (−100°C to 25°C; 25°C to 100°C; −100°C to 100°C). Figure 8a shows that the introduction of lignocellulosic reinforcement contributes to the higher dimensional stability of the original composites over the entire analyzed temperature range compared to the PE matrix. The decrease in thermal expansion is more significant in fibrous composites and particularly in those reinforced with 40% *Arundo* fibres. This seems to be related to the formation of a network of physical interactions between the dispersed fibres

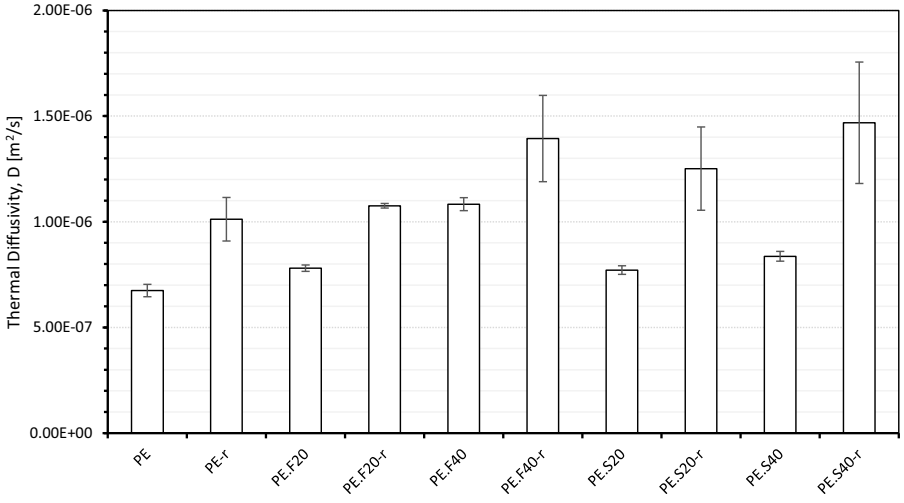

Figure 7: Thermal diffusivity of PE-Arundo composites.

within the matrix that significantly restricts their mobility and greater consistency to create 3D steric hindrances in the sample volume, as described in the previous work [67].

Regarding the recycling effect on the variation of relative length change, reprocessing leads to a slight increase in the dimensional variation of the composites with temperature due to the shortening of the fillers and consequently, a lower restriction in the mobility of the polymer matrix. However, the material with 20% shredded reed shows an opposite behaviour above −16°C. Thus, over the entire temperature range, this formulation (PE.S20-r) shows an almost identical trend to the composites with 20% fibrous filler after reprocessing (PE.F20-r). This is in agreement with the results of the morphological analysis of the composites with a lower proportion of fillers, as well as with the thermo-mechanical performance of both formulations loaded at 20% after recycling. The higher shortening rate of fibres after multiple extrusions leads to an equivalent performance to that of composites made from shredded reed. From this perspective, it can be concluded that the use of shredded reed as reinforcement in low-load composite materials is a more cost-effective option when reprocessing is considered, taking into account the more economical and sustainable nature of its production process [37].

In terms of thermal expansion coefficients, only neat HDPE and the 20% shredded series show a significant reduction in α over the entire temperature range. If we limit the analysis to the most likely temperature range for conventional use (−100°C to 25°C), PE-r shows a reduction in α of 13%, while PE.S20-r reduces this factor by 35%, as shown in Figure 8b. The other formulations keep similar expansion coefficients in this interval even after recycling and expand to a greater extent when the temperature is increased beyond 25°C.

3.4 Mechanical and thermo-mechanical performance

3.4.1 Deflection and softening temperatures

It was found that thermo-mechanical performance evaluated in static load conditions and non-isothermal conditions, such as HDT and VST, were significantly affected by successive reprocessing, as shown in Table 2. Both

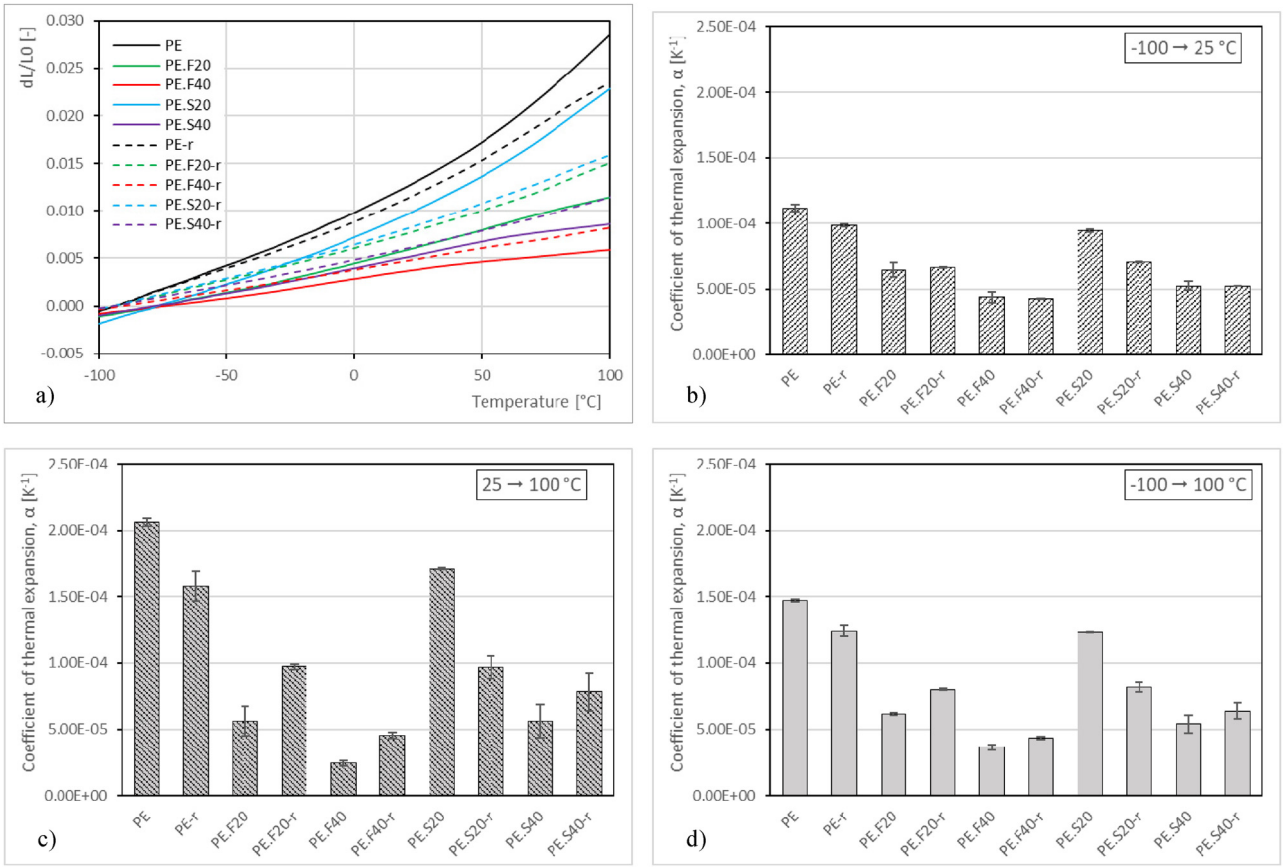

Figure 8: TMA results: (a) changes in length and average coefficients of thermal expansion within temperature intervals of (b) −100°C to 25°C, (c) 25–100°C, and (d) −100°C to 100°C.

Table 2: Average values (±standard deviations) for mechanical and thermo-mechanical properties of HDPE matrix and Arundo composites before and after closed-loop reprocessing

Material	HDT (°C)	VST (°C)	Ball indentation hardness ($N \cdot mm^{-2}$)	Impact strength ($kJ \cdot m^{-2}$)	Tensile properties		Flexural properties		DMTA	
					Ultimate strength (MPa)	Elastic modulus (MPa)	Ultimate strength (MPa)	Elastic modulus (MPa)	E' (10^9 Pa)	B (10^{-9} $Pa^{-1}\%^{-1}$)
PE	41.0 ± 1.3	72.3 ± 1.6	44.0 ± 0.5	6.4 ± 0.1	19.0 ± 0.1	1,058.5 ± 16.9	26.5 ± 0.1	753.1 ± 56.1	1.402	<0.04
PE.F20	57.3 ± 1.3	81.3 ± 1.6	52.0 ± 1.3	7.5 ± 0.2	19.0 ± 0.1	1,881.6 ± 45.1	30.5 ± 0.2	1,538.2 ± 77.9	1.734	0.63
PE.F40	72.9 ± 1.6	85.8 ± 3.0	59.6 ± 2.9	7.1 ± 0.1	17.5 ± 0.1	2,022.8 ± 98.1	30.6 ± 0.2	1,270.7 ± 125.7	1.928	1.36
PE.S20	55.3 ± 2.0	78.9 ± 0.3	49.9 ± 2.0	6.1 ± 0.1	19.0 ± 0.1	1,490.9 ± 28.7	30.6 ± 0.3	1,469.7 ± 23.4	1.659	0.86
PE.S40	67.5 ± 4.7	83.4 ± 1.9	57.3 ± 1.2	5.5 ± 0.2	16.4 ± 0.3	1,675.3 ± 119.4	28.9 ± 0.3	767.8 ± 73.9	1.782	2.08
PE-r	42.4 ± 1.3	72.5 ± 1.2	35.7 ± 0.5	6.5 ± 0.5	21.7 ± 0.1	1,399.5 ± 29.7	31.3 ± 0.4	931.4 ± 43.1	1.874	<0.04
PE.F20-r	52.2 ± 0.4	75.2 ± 1.0	39.1 ± 0.9	6.3 ± 0.0	19.4 ± 0.0	2,003.5 ± 53.3	33.0 ± 0.3	2,088.2 ± 51.9	2.458	0.23
PE.F40-r	66.0 ± 0.2	76.3 ± 1.0	44.3 ± 0.5	5.7 ± 0.1	18.3 ± 0.1	2,919.9 ± 121.8	35.1 ± 0.2	2,935.5 ± 77.3	2.598	0.88
PE.S20-r	50.1 ± 1.0	74.7 ± 1.1	38.8 ± 0.9	4.8 ± 0.1	19.2 ± 0.2	1,914.8 ± 58.9	33.8 ± 0.2	1,778.1 ± 48.6	2.161	0.36
PE.S40-r	59.1 ± 0.1	76.6 ± 1.7	43.4 ± 0.9	4.9 ± 0.1	18.0 ± 0.1	2,542.2 ± 54.8	34.8 ± 0.5	2,359.9 ± 155.1	2.434	0.89

Tukey tests were used to compare the properties of the different material groups with a 95% confidence level. *P*-values for the pairwise comparison of each property are reported in the Supplementary Material section (Tables S1–S8).

properties are reduced after recycling for all series, starting to deform under load at lower temperatures (between 4.2°C and 9.4°C below), with the effect being more noticeable in composites with higher lignocellulosic filler loadings. This effect is consistent with the results reported by Bhattacharjee and Bajwa [50], where a similar trend in the evolution of thermo-mechanical properties after six reprocessing cycles of HDPE-based composites was found, but contrasts with the results of the same authors regarding the effects of continuous recycling on the remaining stiffness properties: tensile modulus, flexural modulus, and storage modulus.

3.4.2 Mechanical properties

Figure 9 shows an overview of the variation in the mechanical properties of the original and reprocessed materials. If we look at the stiffness under quasi-static tensile and bending tests at room temperature, increases of up to 50% and 200%, respectively, are observed for the PE.S40-r series. Similar rigidity gains, even at higher absolute values, are achieved for composites with 40% fibres. Meanwhile, recycled materials with lower biomass content are also moderately stiffer (up to 30% in flexural modulus). Ultimate tensile and flexural strength results are as well slightly above the initial values for all series, with all variations being statistically significant as a function of both the type and the amount of filler following analysis of variance and Tukey's post hoc tests (Supplementary Material). The stiffening in recycled composites is mainly due to the predominance of cross-linking reactions in the polymer matrix structure [68] since no improvement in phase bonding was observed as a result of thermo-mechanical reprocessing following the adhesion factor (A) calculated from the DMTA tests.

The increased cellulose filler content contributes to the stiffening of the polymeric material in the original composites with both types of fillers as a result of the distribution of stiff filler structures in the boundary layer [38]. The recycling process leads to a further increase of this property for all series due to the increase in the rigidity of the matrix. It is observed that the elastic modulus for the original material is more dependent on the type of filler, while this trend changes for the recycled materials. This is presumably a consequence of the smaller size of the rigid particles and the lower aspect ratio of the fibres, which explains the reduced difference in the elastic modulus between fibres and shredded samples series. Therefore, the aspect ratio has a more pronounced impact on stiffness than the type of filler. Regarding the impact strength, the results of the prior research indicating that a higher MFI lowers the toughness of composites [69] are supported by the correlation between increased flowability and lower impact

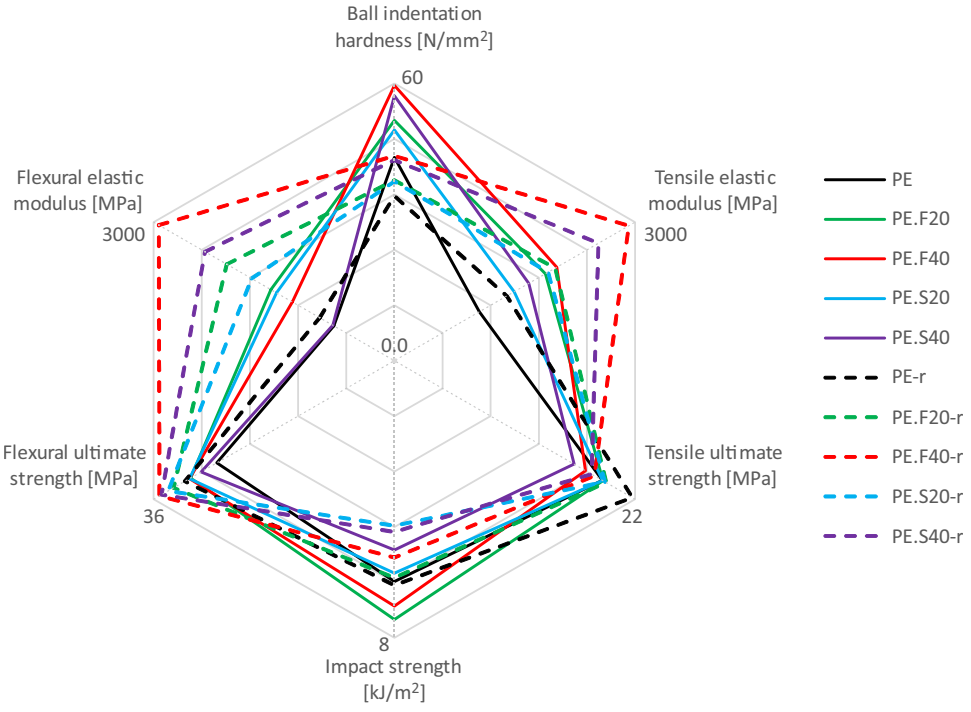

Figure 9: Overall results on the mechanical properties of the original and reprocessed materials.

resistance after reprocessing. As in the first injection moulding, composites with fibrous fillers have higher impact strength than those with shredded material after reprocessing.

3.4.3 DMTA

DMTA provides valuable information on the viscoelastic behaviour of thermoplastic composites at different temperatures and loading rates. By measuring dynamic parameters such as storage modulus (E'), loss modulus (E''), and damping factor (Tan δ), which are temperature dependent and reveal insights into the interfacial bonding between the fillers and polymer matrix, it is possible to emphasize the rheological behaviour of NFC in terms of energy dissipation under cyclic load [70].

During the first moulding (cycle 0), it was found that all composite series produced higher storage modulus than neat HDPE, meaning that plant fillers stiffen the matrix over the studied temperature window [38]. After the reprocessing (cycle 6), the composites, as well as the PE matrix, undergo an even greater rise in storage moduli that reach average values 64% higher than those of the original

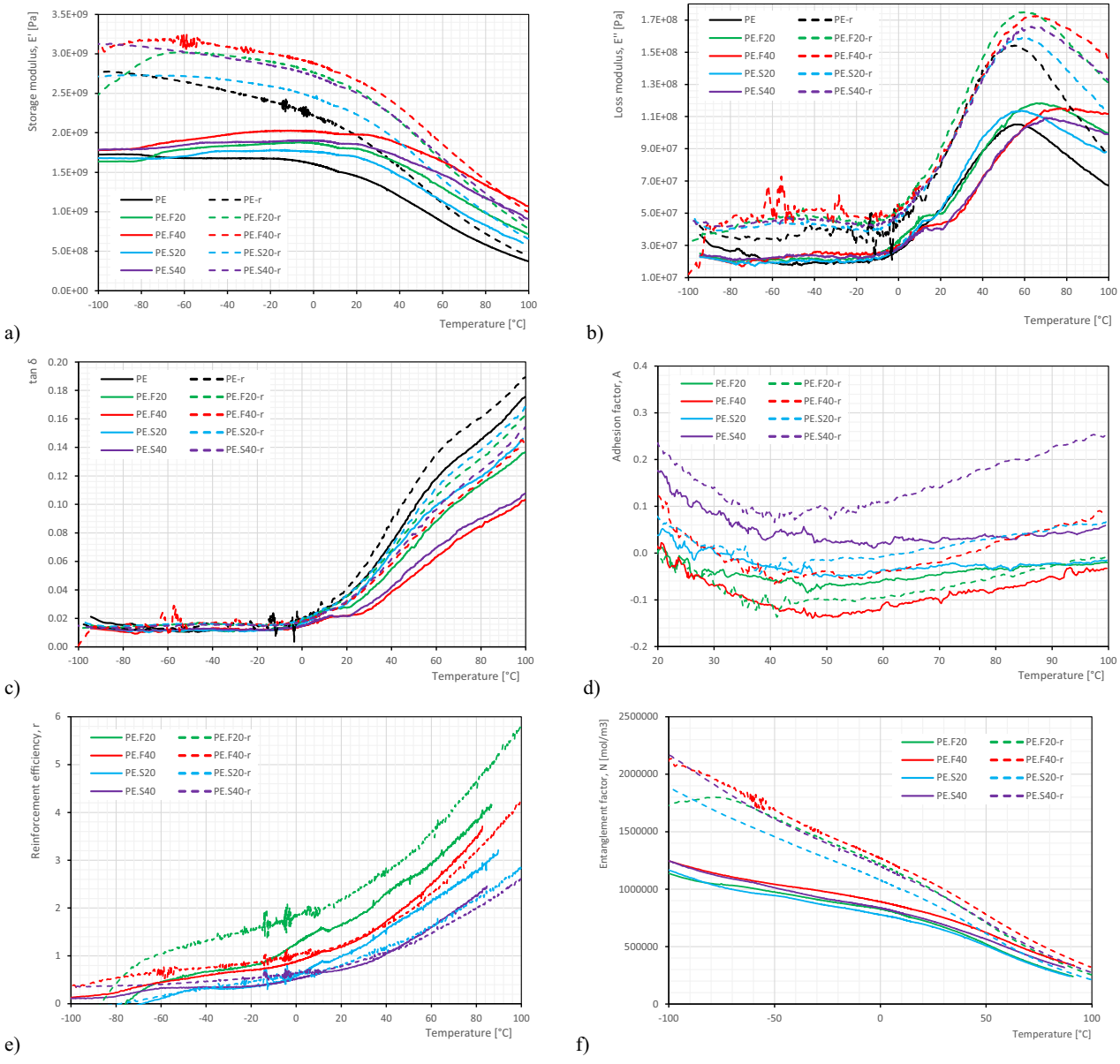

Figure 10: Variation of (a) storage modulus, (b) loss modulus, (c) loss factor, (d) adhesion factor, (e) entanglement factor, and (f) reinforcement efficiency from DMTA.

materials at −60°C, increased by 49% at −20°C and 37% above at 20°C (Figure 10a). It is worth noting that, compared to the initial processing stage, after recycling, the type of filler is more decisive in the evolution of storage modulus than the loading amount for the range of temperatures studied. The defibrillation and entanglement of the reed fibres within the matrix favour stress transmission largely than the irregularly shaped particles of the shredded filler.

Both the recycled *Arundo* composites and HDPE matrix show higher loss moduli than the original materials (Figure 10b), which means that reprocessing provides a lower elastic recovery and a more predominantly viscous behaviour, as observed in the rheological analysis. Maximum loss modulus values occur at about 60°C for all recycled series, with the higher loading composites shifting this value about 7°C lower compared to the first processing cycle. This temperature represents the α-relaxation, associated with an interlamellar shear process of HDPE, which is usually in the range from 20°C to 70°C [71]. This peak in E'' curve corresponds to the transformation from the rigid phase to the viscous state and represents the highest service temperature for composite applications, which is consistent with the results observed from the HDT and VST tests.

The α-transition is also observed as an inflection in the curves in tan δ plots (Figure 10c). Loss factor curves show another inflection point between 0°C and 10°C, which can be attributed to the slippage or relaxation of the crystalline regions in PE, rather than the glass transition of the amorphous regions [72,73]. Although no significant variation of loss factor was observed in the temperature range from −100°C to this inflection point, all series show an increase in tan δ beyond it. This trend is opposite to that found by Ramzy [74] when recycling hemp and sisal reinforced PP composites and indicates a deterioration in fatigue performance of HDPE-*Arundo* composites after recycling.

The brittleness (B) of the different formulations at 25°C is reduced by about 60% for all composites, except for the PE.F40-r series, which only improves this mechanical property by about a third as shown in Table 2. The main reason for this different behaviour is the lower increase in ductility for materials with 40% fibre content after thermo-mechanical processing. The elongation at break (ε_b) of the PE.F40-r series is only 15% higher than that of PE.F40, while the other composites can achieve elongations 70–90% longer compared to the original materials. The relative increase of the entanglement factor together with the higher stiffness of the fibres, in a higher weight ratio, might explain the lower change in the stretchability of these samples despite the reduction in the fibre size.

The adhesion of reinforcing materials in NFC depends on the affinity between the phases. It is well known that polyolefins have a nonpolar and hydrophobic character, and a difference in polarity with respect to plant fibres causes a deterioration of mechanical properties of composites [75]. Since lower values of A indicate higher interfacial adhesion [76], it can be deduced from Figure 10c that this condition is only met when reprocessing 20% fibre material. The remaining reed composites seem to show weaker adhesion after reprocessing. This could be due to thermo-oxidative degradation of cellulose fillers over multiple reprocessing cycles as demonstrated by Fonseca-Valero et al. [49].

Entanglement factor (n) and reinforcement efficiency (r) have been also used to assess the degree of intertwining of fibres within the matrix and how effectively the plant fillers enhance the composite's strength. As with the original material, fibre composites with lower loading have the highest intertwining factor after the closed-loop recycling process (Figure 10e), which could be related to the more brittle character described earlier. In terms of reinforcement efficiency, the better mechanical performance of the fibrous composites is once again confirmed, being the 20% the only series providing a clear positive change after reprocessing in reinforcement efficiency, while the entanglement factor increases for all composites due to the higher homogeneity achieved.

3.5 Morphological analysis

3.5.1 WAXS

Figure 11 shows X-ray diffraction patterns of the PE and its composites obtained by injection moulding before (black line) and after six reprocessing cycles (red line). In the case of all WAXS patterns, characteristics for PE reflections at 21.4°, 23.8°, 29.3°, and 36.2° are observed, which correspond to crystal planes (110), (200), (210), and (020) results from the orthorhombic characteristic of crystalline structure developed in the polymer [77,78]. In the case of pure PE, additional diffraction reflection is observed in the plane (010) at 19.4°, corresponding to the developed monoclinic phase [78]. Taking into account the diffractometric characteristics of the used filler described in our earlier work [37], the change in the shape of the WAXS pattern of composite samples is justified. In the case of shredded and fibrous reed-based fillers, broad diffractometric peaks with a maximum at 2Φ = 22–23° are observed at (002) crystallographic plane originated from cellulose I [79] and (101), attributed

to crystalline cellulose phase [80]. In the case of composite materials, the maximum intensity of the diffraction peaks was limited; the higher the filler content, the lower it was. This effect was more pronounced for the shredded material. The sixfold reprocessing increased the intensity of the observed diffractometric peaks for all the given materials. Figure 12 presents the crystallinity values calculated according to Eq. 2. The introduction of lignocellulose fillers reduced the crystallinity of the original materials. These results are in line with those reported by Sewda and Maiti [81]. However, it should be considered that the external layer of the materials formed was studied at very high cooling and shear rates, which may influence the crystalline structure at the sample surface due to the effects of frozen-in molecular elongation and lamellae orientation [82]. Moreover, solidification conditions different from

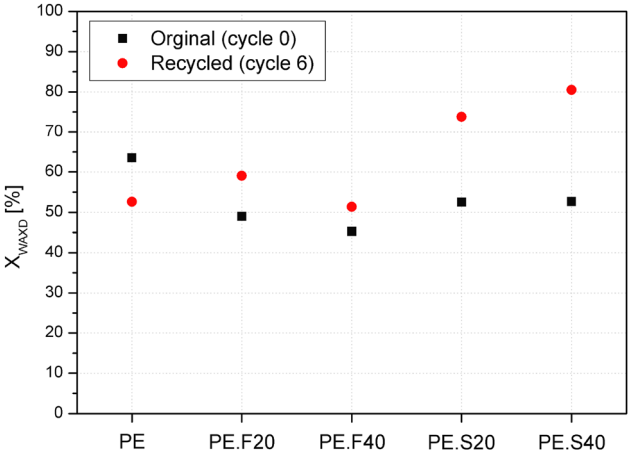

Figure 12: WAXS-based crystallinity of PE and its composites before and after reprocessing.

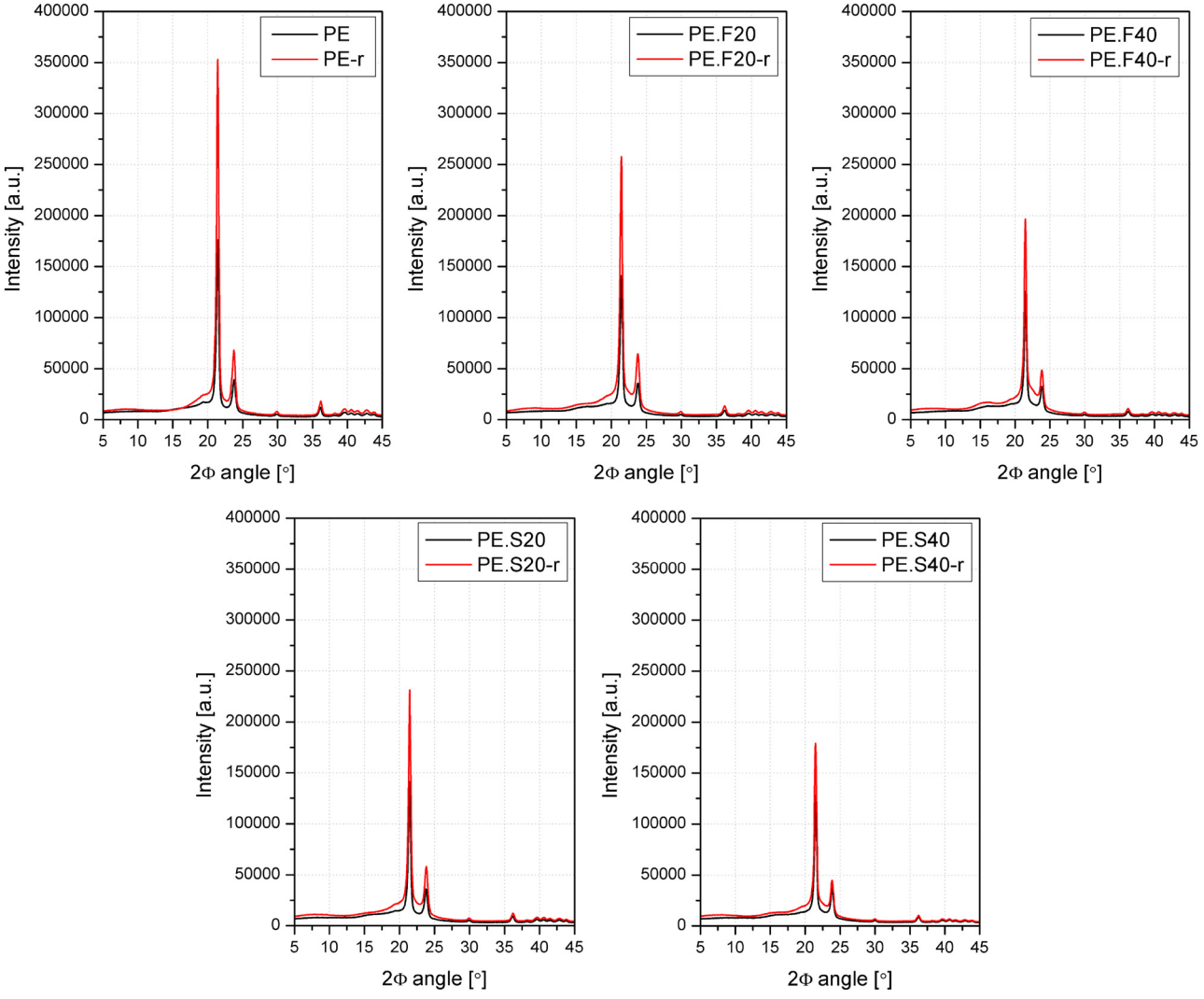

Figure 11: WAXS patterns of original (cycle 0) and recycled (cycle 6) PE and its composites.

those in the case of samples tested by DSC may provide differences in the values determined by those analytical techniques. Considering the determined crystallinity based on diffractometric analysis results (Figure 12), an opposite trend can be observed in the case of pure PE and composites in the change of the degree of crystallinity induced by reprocessing, which is in line with the DSC results from the first heating. In the case of PE, reprocessing probably caused an intensive chain scission phenomenon, leading to the shortening of macromolecules and, due to degradative changes, an increase in the share of amorphous domains. The phenomenon of partial shortening of main PE chains probably also took place in the case of reed-filled materials. However, in this case, the effect of increasing crystallinity is observed. It suggests that macromolecules with lower molecular weight were more susceptible to heterogeneous nucleation caused by dispersed polymeric matrix fillers.

3.5.2 Particle size assessment

Filler size and distribution are some of the most influential parameters on both the mechanical performance, water uptake and thermal behaviour of short fibre-reinforced polymer composites. Figure 13 shows how the aspect ratio of *Arundo* fibres decreases after reprocessing, while for shredded reed it remains largely unchanged at lower values. The variation in aspect ratio is a consequence of shortening of the fibre length due to mechanical reprocessing; this is reduced, on average, by a quarter of its initial length. A similar length variation was reported by Lila et al. after five cycles of extrusion and injection moulding on bagasse fibre-reinforced PP [83]. The diameter of the fibrous filler remains practically unchanged at around 125 microns, as an average value. Benoit, in her study on long-term closed-loop recycling of HDPE/flax composites, found that fibre breakage occurs primarily during the first cycles [57]. After a few reprocessing cycles, there is no significant variation in either length or aspect ratio, although a decrease in standard deviation is noted, indicating that the distribution tends to become smaller with recycling.

On the other hand, the shredded filler undergoes size changes of the same order of magnitude in both length and diameter. For this reason, the aspect ratio of the irregularly shaped particles remains practically unchanged. The lower reinforcement efficiency and impact strength of the recycled shredded composites in comparison to the fibrous ones can be explained by this difference in fillers size and aspect ratio, as for the first injection moulding.

3.5.3 Density and porosity

The increased fibre content in PE-based composites generally results in higher density due to the mass contribution of the lignocellulosic fibres. However, it is reasonable to expect that the effective density might drop in comparison to the original composite if the plant fillers deteriorate during reprocessing. This effect could be accentuated in cases where the surface and interfacial areas become compromised, resulting in weaker bonds. Thus, according to some studies found in the literature, reprocessing can lead to a reduction in the overall density of HDPE-based composites due to the degradation of raw materials, especially when the reinforcing cellulose fillers lose their structural integrity and decrease in crystallinity over successive processing cycles [68,84].

In this case, as expected due to the density of the fillers, the more the lignocellulosic material in the composite, the higher the density measured. However, when comparing

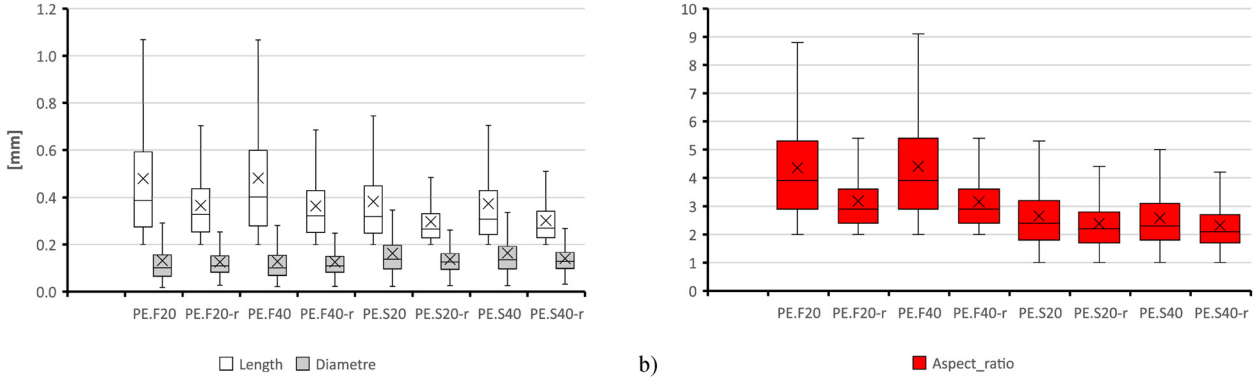

Figure 13: Variations in (a) length and diameter and (b) aspect ratio of filler particles due to reprocessing.

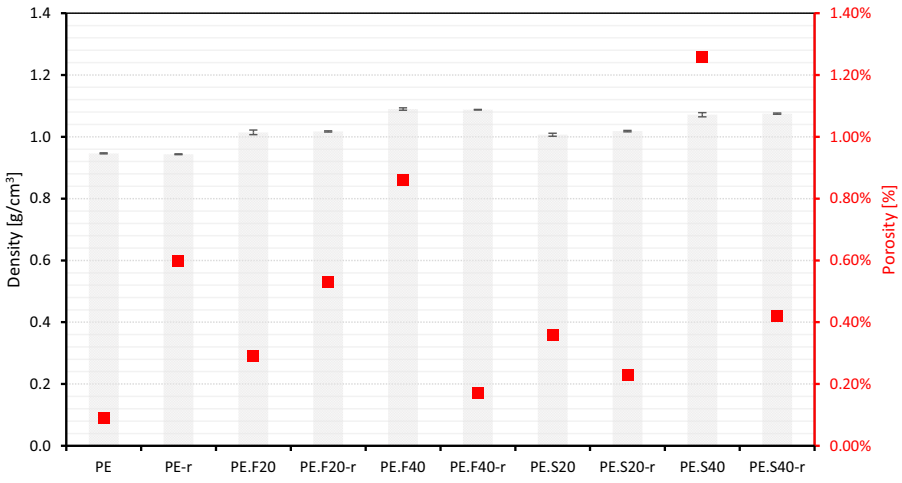

Figure 14: Average density and porosity of original vs recycled materials.

the density of injection-moulded samples in cycle 0 and cycle 6, almost identical specific weights were measured before and after recycling each material formulation, for both fibres and shredded reed fillers. This is consistent with the density progression reported on long-term closed-loop recycling of HDPE/flax composites, in which negligible fluctuations of density were also observed [57]. It should be mentioned that, in the present work, the original and reprocessed materials were moulded using the same injection process parameters. Therefore, the lower MFI in the recycled composites might have influenced the compactness of the samples.

An increase in porosity due to the breakdown of fibre structures, which could create gaps in the matrix, is another possible effect of composites reprocessing. The presence of voids not only affects the mechanical attributes but also the physical properties such as density or hygroscopicity. The porosity in Figure 14 is determined by X-ray tomography on injection-moulded samples (80 mm long, 10 mm wide, and 4 mm thick). The most significant variations in the amount of trapped air voids were observed for the 40% filler samples, with a reduction in the pore volume of nearly 0.8% after five cycles of extrusion reprocessing and subsequent injection moulding of the composites (Figure 15).

3.6 Water absorption

Despite the hydrophobic nature of HDPE, which generally saturates to less than 1% without significant swelling, NFC

Figure 15: 3D computed tomography images presenting pores distribution.

based on this type of thermoplastic matrix may present a high level of water uptake influenced by the presence of pores, gaps between the polymer and the reinforcing phase, or micro-cracks affecting the water permeability within the matrix/filler [27,62].

By adding plant fibres to the polymer matrix, the water absorption capacity of NFC is significantly increased. This is mainly due to the hydrophilic nature of lignocellulosic fibres, which makes these materials more susceptible to swelling and dimensional instability. On the other hand, reprocessing significantly influences the water absorption properties of composite materials, particularly those reinforced with natural fibres. Some research works indicate that with each successive reprocessing cycle, the water absorption rate and capacity of composites tend to decrease [85]. For instance, a study on mechanical recycling of biobased PE-agave fibre composites found a reduction of approximately 11% in maximum water absorption capacity between the first and fourth cycles [86]. The smaller size of the fibres and their better dispersion within the matrix as the number of cycles increases are responsible for this decrease, as they improve the encapsulation of the filler and reduce the voids between the two phases of the composite.

Figure 16 shows the water absorption during 4 weeks of immersion in distilled water at room temperature for moulded parts made from the different studied materials in cycle 0 and cycle 6. Maximum water absorption typically occurs over long periods; González-Aguiar reported a time of 1,000–1,200 h for saturation of PE biocomposites with up to 50% agave fibres [86]. Apart from neat HDPE, which has negligible absorption rates, the composites with the lowest amounts of filler, PE.F20-r, and PE.S20-r, were the first to reach the equilibrium point with a saturation level of around 1% after barely 2 weeks, which is 55% and 41% less than before reprocessing, respectively. Meanwhile, the PE.S40-r series is the one that shows the greatest decrease in the water uptake, going from a maximum absorption of over 8% after a month of soaking for the original material to only 3.3%. The fibrous composite with the highest loading amount, on the other hand, also reduces its absorption capacity, but only by one-third compared to the initial value.

Table 3 shows the variation of other parameters related to the hygroscopicity and kinetics of water absorption, such as the Fick diffusion coefficient, swelling, sorption, or permeability. Regarding the swelling of the samples at the end of the test, the trend is similar to that found for water uptake. The composite with 40% reed fibre shows the greatest thickening variation before and after recycling. Except for this sample series, the reduction in swelling is about half compared to the original material.

All samples followed a Fickian-type behaviour with diffusion coefficients in the recycled materials slightly higher than those obtained in the first injection moulding. Water sorption shows the ratio between the mass of water absorbed by the sample and the weight of the sample itself, considering both diffusion and percolation mechanisms. It was found that water sorption capacity depends mainly on the amount of *Arundo* filler. While there is no difference after recycling between composites with 20% fibre or shredded composite, in those with 40% reed, fibre composites show the highest sorption level. Regarding the permeability, obtained by the combination of sorption and

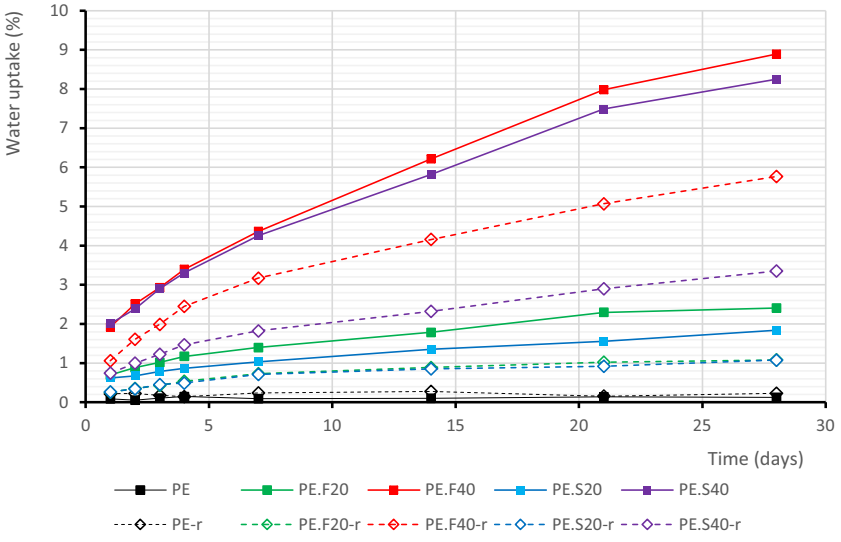

Figure 16: Evolution of water uptake vs time for the original and the reprocessed materials.

Table 3: Variation of water uptake parameters

Material	k (%/s$^{0.5}$)	D (m^2·s^{-1})	n	Swelling (%)	Sorption (g·g^{-1})	Permeability (m^2·s^{-1})
PE	3.53×10^{-5}	2.62×10^{-13}	0.12	1.1	0.001	3.44×10^{-16}
PE.F20	1.61×10^{-3}	3.56×10^{-13}	0.36	3.3	0.024	8.52×10^{-15}
PE.F40	4.98×10^{-3}	2.70×10^{-13}	0.40	8.3	0.089	2.40×10^{-14}
PE.S20	1.10×10^{-3}	2.84×10^{-13}	0.29	2.3	0.018	5.22×10^{-15}
PE.S40	4.88×10^{-3}	2.90×10^{-13}	0.38	6.6	0.083	2.39×10^{-14}
PE-r	1.10×10^{-4}	2.91×10^{-13}	0.06	0.5	0.002	6.82×10^{-16}
PE.F20-r	8.09×10^{-4}	4.40×10^{-13}	0.33	1.4	0.011	4.76×10^{-15}
PE.F40-r	3.86×10^{-3}	3.50×10^{-13}	0.42	5.5	0.058	2.02×10^{-14}
PE.S20-r	6.29×10^{-4}	2.70×10^{-13}	0.25	1.2	0.011	2.92×10^{-15}
PE.S40-r	2.19×10^{-3}	3.36×10^{-13}	0.41	3.0	0.034	1.13×10^{-14}

diffusion attributes, it is interesting to note that despite a worsening of this property for the HDPE matrix, all composites show a reduction in permeability after the closed-loop reprocessing. These results are comparable to those reported by Jubinville when analyzing HDPE-based composites reinforced with hemp hurd. In this study, it was found that beyond 15% loading, the absorption kinetics of the cellulosic phase becomes more important than that of the matrix. Composites with 50% hemp showed the highest diffusion and permeability coefficients due to the incapacity of the matrix to efficiently encapsulate the hydrophilic material and contain moisture penetration [62].

3.7 Colour and gloss evaluation

Reprocessing often leads to significant changes in the visual appearance of NFC. For instance, a gradual shift from original colours to yellowish or darker can occur due to thermal degradation and oxidation processes during recycling.

An overview of the colour and gloss assessment is shown in Table 4. Taking as reference the colour of the original moulded samples (cycle 0), noticeable colour changes were appreciated for all reprocessed series, resulting in a less vibrant and more muted colour appearance, in line with the trend reported by other biocomposites recycling studies in the literature [86,87]. A decrease in the parameter ΔL^* (lightness) is related to the darkening of the samples, while negative values of Δa^* (red/green coordinate) indicate a trend from red to greener colours and Δb^* (yellow/blue coordinate) below zero denotes a shift from yellow to blue hues. Although both composites and recycled HDPE show total colour differences (ΔE) of comparable magnitude, PE-r series mainly varies in shade, keeping hues with similar values to those of the original material. The most significant change colour coordinates occur in the shredded *Arundo* composites, which change from a more yellowish hue in the original compounding to a more bluish colour after reprocessing.

Gloss is the visual perception of direct light reflected from a surface that is associated with perceived brightness.

Table 4: Colour and gloss changes

Material	Colour							Gloss		
	L^*	a^*	b^*	ΔL^* [(1)]	Δa^* [(1)]	Δb^* [(1)]	ΔE [(1)]	20°	60°	85°
PE	72.47 ± 0.13	−0.91 ± 0.03	−0.31 ± 0.12	–	–	–	–	27.4 ± 3.5	69.0 ± 5.2	84.7 ± 2.2
PE.F20	56.26 ± 0.88	12.37 ± 0.46	23.67 ± 0.94	−16.21	13.28	23.98	31.845	1.0 ± 0.2	7.8 ± 1.1	8.5 ± 2.8
PE.F40	58.37 ± 1.42	12.00 ± 0.71	26.16 ± 1.40	−14.10	12.91	26.47	32.651	1.1 ± 0.5	7.6 ± 3.0	17.4 ± 5.6
PE.S20	41.61 ± 1.27	5.32 ± 0.30	18.77 ± 0.64	−30.86	6.23	19.08	36.810	7.1 ± 1.0	32.4 ± 3.2	53.9 ± 3.0
PE.S40	49.33 ± 1.52	4.44 ± 0.25	15.61 ± 1.02	−23.14	5.36	15.92	28.593	3.0 ± 1.0	18.2 ± 4.3	35.5 ± 7.5
PE-r	62.32 ± 0.11	−1.18 ± 0.03	−0.12 ± 0.07	−10.15	−0.27	0.19	10.154	31.7 ± 1.7	74.6 ± 2.3	89.1 ± 2.8
PE.F20-r	45.27 ± 0.61	10.08 ± 0.40	20.12 ± 0.70	−11.00	−2.29	−3.55	11.778	2.6 ± 0.6	17.1 ± 1.5	25.7 ± 3.9
PE.F40-r	49.92 ± 1.33	10.56 ± 0.52	19.71 ± 1.30	−8.45	−1.44	−6.45	10.725	0.9 ± 0.4	7.3 ± 3.4	13.5 ± 5.9
PE.S20-r	36.24 ± 1.30	2.45 ± 0.42	10.04 ± 0.66	−5.37	−2.87	−8.73	10.648	2.5 ± 0.3	17.5 ± 1.0	26.5 ± 5.6
PE.S40-r	38.25 ± 3.08	2.31 ± 0.42	8.55 ± 0.88	−11.08	−2.13	−7.06	13.308	1.9 ± 0.7	14.1 ± 1.0	24.4 ± 8.0

[(1)] Differences in colour calculated with respect to neat HDPE in cycle 0 and with respect to unrecycled equivalents in cycle 6.

High reflectance surfaces are referred to as glossy; while semi-gloss or matt surfaces are less reflective. Considering the variety of gloss found among the different samples, the standard measurement at 60° was complemented by measurements at an angle of 20° for high gloss surfaces (values above 70 GU) and at 85° for matt surfaces (values below 10 GU). In the first moulding, it was observed that the fibre composites provided a matt surface with lower gloss than the shredded reed ones. And among the latter, the gloss decreased with the increasing filler content. The most noticeable variation observed after recycling was in the PE.F20-r series, with a marked increase in gloss. This is possibly caused by the smoother surface produced by the reduction in fibre size and a more uniform distribution of the filler. For shredded composites, a rougher surface finish after the final injection moulding results in a decrease in reflectivity. Mechanical attrition of irregularly shaped particles during reprocessing may contribute to this change. As the particles break down, the surface texture of the composite changes, which may scatter light more diffusely rather than reflect it in a specular manner.

4 Conclusions

Despite small losses in thermo-mechanical properties, the study reveals that HDPE-Arundo composites exhibit a worthy level of sustainability, with some improvements in processability and mechanical performance after closed-loop recycling using co-rotating twin-screw extrusion. These characteristics allow for reuse and reprocessing, prolonging the durability of such resources.

FTIR spectroscopy reveals minor variations in chemical composition between the original and the recycled materials. HDPE-based composites show resistance to oxidation, as seen in the persistence of C–H peaks, while some C–O groups in the fingerprint region, related to cellulose, weaken after recycling.

Adding Arundo fillers to the HDPE matrix does not hinder processing and may even improve it. After five-cycle reprocessing, all materials tend to increase their MFI slightly, most noticeably for biocomposites with shredded reed fillers. After that, the most loaded fibrous compound only need 40% higher moulding pressure than pure HDPE. The lack of adhesion promoters in the compounding phase seems to favour a trend towards improving processability and some aspects of mechanical performance rather than degrading the materials throughout the recycling process. Oscillatory rheology revealed that fibrous composites increase complex viscosity, while shredded ones decrease it. All formulations keep their viscous character, with higher loss moduli than storage moduli. Capillary rheology confirmed that the flow resistance mainly depends on the filler amount, regardless of type.

Thermogravimetric analysis proved thermal stability up to 40°C above processing temperature by injection moulding. Melting temperatures remain consistent around 135°C, while crystallization temperatures slightly increase by less than 5°C for recycled formulations. Arundo-filled materials show an increase in the enthalpies of fusion and crystallization of between 20% and 40% and a small increase in crystallinity. Despite the initial contribution of reed fillers to the OIT, multiple reprocessing led to a drop in OIT for all materials by more than half compared to the PE matrix, except for the PE.F20-r series, which manages to contain it at only 20% less.

HDT and VST decrease after recycling up to a maximum of 9°C, especially in composites with higher lignocellulose loading. On the contrary, reprocessed materials rise their stiffness, in both flexural and tensile elastic moduli, because of the cross-linking reactions typical of PE, and without any enhancements in the inter-phase adhesion being observed. Impact strength is negatively affected by the shortening of the filler length, which results in a one-quarter reduction in aspect ratio after reprocessing in the case of reed fibres. However, tensile and flexural strength increase by up to 10% and 20%, respectively, due to improved fibre intertwining highlighted by entanglement factor and reinforcement efficiency. PE.S40-r was the series that showed the greatest increase in mechanical properties after reprocessing, approaching in performance that of the comparatively more expensive 40% reed fibres composite. All reprocessed materials become tougher, while neat HDPE and 40% filled composites also significantly increase their resilience.

DMTA study found that plant fillers stiffen the HDPE matrix even more after reprocessing, resulting in a higher storage modulus where the type of filler is more crucial than the filler load. The recycled materials exhibit higher loss moduli, suggesting a shift towards more viscous behaviour. An inflection point in the loss factor above 0°C points to a worsening of fatigue performance after recycling. Brittleness at room temperature is decreased by 60% in most composites, extending the elongation at break up to 90% beyond the original values, with the exception of the PE.F40-r series, which becomes slightly less ductile than the others.

No significant changes in the density and porosity of the recycled composites were observed. However, lower water absorption was confirmed, possibly due to smaller

fillers and more uniform distribution after reprocessing, reducing interphase voids in the composite through improved filler encapsulation. Finally, colour and gloss assessments showed noticeable changes in visual appearance for all reprocessed series, resulting in less vibrant colours and shredded composites having lower gloss than fibre composites.

Acknowledgments: Luis Suárez: Ph.D. grant program co-financed by the Canarian Agency for Research, Innovation and Information Society of the Canary Islands Regional Council for Employment, Industry, Commerce and Knowledge (ACIISI) and by the European Social Fund (ESF) (Grant number TESIS2021010008). LICEM project (EIS 2021 33), funded by Consejería de Economía, Conocimiento y Empleo, Gobierno de Canarias, through FEDER funds (Canarias Avanza con Europa).

Funding information: The authors state no funding involved.

Author contributions: Luis Suárez: methodology, formal analysis, investigation, visualization, and writing – original draft preparation; Mateusz Barczewski: conceptualization, methodology, investigation, formal analysis, and writing – reviewing and editing; Mark Billham: investigation, resources, and writing – reviewing and editing; Andrzej Miklaszewski: investigation and writing – reviewing and editing; Patryk Mietliński: investigation; Zaida Ortega: conceptualization, methodology, investigation, resources, writing – reviewing and editing, and supervision. All authors read and approved the final manuscript.

Conflict of interest: The authors state no conflict of interest.

Data availability statement: The datasets generated during and/or analysed during the current study are available from the corresponding author on reasonable request.

References

[1] Kumar R, Ul Haq MI, Raina A, Anand A. Industrial applications of natural fibre-reinforced polymer composites–challenges and opportunities. Int J Sustain Eng. 2019;12(3):212–20.

[2] Praveena BA, Buradi A, Santhosh N, Vasu VK, Hatgundi J, Huliya D. Study on characterization of mechanical, thermal properties, machinability and biodegradability of natural fiber reinforced polymer composites and its Applications, recent developments and future potentials: A comprehensive review. Mater Today Proc. 2022;52:1255–9.

[3] Rajeshkumar L, Kumar PS, Ramesh M, Sanjay MR, Siengchin S. Assessment of biodegradation of lignocellulosic fiber-based composites – A systematic review. Int J Biol Macromol. 2023;253:127237.

[4] Usman MA, Momohjimoh I, Gimba ASB. Effect of groundnut shell powder on the mechanical properties of recycled polyethylene and its biodegradability. J Min Mater Charact Eng. 2016;4(3):228–40.

[5] Zhao X, Copenhaver K, Wang L, Korey M, Gardner DJ, Li K, et al. Recycling of natural fiber composites: Challenges and opportunities. Resour Conserv Recycl. 2022;177:105962.

[6] Ortega Z, Bolaji I, Suárez L, Cunningham E. A review of the use of giant reed (*Arundo donax* L.) in the biorefineries context. Rev Chem Eng. 2024;40(3):305–28.

[7] Suárez L, Ortega Z, Barczewski M, Cunningham E. Use of giant reed (*Arundo donax* L.) for polymer composites obtaining: a mapping review. Cellulose. 2023;30(8):4793–812.

[8] Corno L, Pilu R, Adani F. *Arundo donax* L.: A non-food crop for bioenergy and bio-compound production. Biotechnol Adv. 2014;32(8):1535–49.

[9] Fernando AL, Barbosa B, Costa J, Papazoglou EG. Giant reed (*Arundo donax* L.): A multipurpose crop bridging phytoremediation with sustainable bioeconomy. Bioremediation and Bioeconomy. Elsevier; 2016. p. 77–95. doi: 10.1016/B978-0-12-802830-8.00004-6.

[10] Coppa E, Astolfi S, Beni C, Carnevale M, Colarossi D, Gallucci F, et al. Evaluating the potential use of Cu-contaminated soils for giant reed (*Arundo donax*, L.) cultivation as a biomass crop. Env Sci Pollut Res. 2020;27(8):8662–72.

[11] Bonfante A, Impagliazzo A, Fiorentino N, Langella G, Mori M, Fagnano M. Supporting local farming communities and crop production resilience to climate change through giant reed (*Arundo donax* L.) cultivation: An Italian case study. Sci Total Env. 2017;601–602:603–13.

[12] Di Fidio N, Antonetti C, Galletti AMR. Microwave-assisted cascade exploitation of giant reed (*Arundo donax* L.) to xylose and levulinic acid catalysed by ferric chloride. Bioresour Technol. 2019;293:122050.

[13] Barreca F, Martinez Gabarron A, Flores Yepes JA, Pastor Pérez JJ. Innovative use of giant reed and cork residues for panels of buildings in Mediterranean area. Resour Conserv Recycl. 2019;140:259–66.

[14] Ferrandez-Villena M, Ferrandez-Garcia A, Garcia-Ortuño T, Ferrandez-Garcia CE, Ferrandez Garcia MT. Properties of wood particleboards containing giant reed (*Arundo donax* l.) particles. Sustainability. 2020;12(24):1–10.

[15] Manniello C, Cillis G, Statuto D, Di Pasquale A, Picuno P. Experimental analysis on concrete blocks reinforced with *Arundo donax* fibres. J Agric Eng. 2022;53(1). doi: 10.4081/jae.2021.1288.

[16] Alshaal T, Elhawat N, Domokos-Szabolcsy É, Kátai J, Márton L, Czakó M, et al. Giant reed (*Arundo Donax* L.): A green technology for clean environment. In Phytoremediation: Management of environmental contaminants. Vol. 1, Cham: Springer; 2015. p. 1–20. doi: 10.1007/978-3-319-10395-2_1.

[17] Galletti S, Cianchetta S, Righini H, Roberti R. A Lignin-Rich Extract of Giant Reed (*Arundo donax* L.) as a Possible Tool to Manage Soilborne Pathogens in Horticulture: A Preliminary Study on a Model Pathosystem. Horticulturae. 2022;8(7):589.

[18] Mavrogianopoulos G, Vogli V, Kyritsis S. Use of wastewater as a nutrient solution in a closed gravel hydroponic culture of giant reed (*Arundo donax*). Bioresour Technol. 2002;82(2):103–7.

[19] Dai L, Lata S, Cobb K, Zou R, Lei H, Chen P, et al. Recent advances in polyolefinic plastic pyrolysis to produce fuels and chemicals. J Anal Appl Pyrolysis. 2024;180:106551.
[20] Janssens V. Plastics – the Facts 2022. Plast Eur. 2022;81. https://plasticseurope.org/knowledge-hub/plastics-the-facts-2022.
[21] Faust K, Denifl P, Hapke M. Recent advances in catalytic chemical recycling of polyolefins. ChemCatChem. 2023;15(13):e202300310.
[22] Khanam PN, AlMaadeed MAA. Processing and characterization of polyethylene-based composites. Ad Manuf: Polym Compos Sci. 2015;1(2):63–79.
[23] Douiri L, Jdidi H, Kordoghli S, El Hajj Sleiman G, Béreaux Y. Degradation indicators in multiple recycling processing loops of impact polypropylene and high density polyethylene. Polym Degrad Stab. 2024;219:110617.
[24] Benoit N, González-Núñez R, Rodrigue D. High density polyethylene degradation followed by closedloop recycling. Prog Rubber, Plast Recycl Technol. 2017;33(1):17–37.
[25] Dugvekar M, Dixit S. High density polyethylene composites reinforced by jute fibers and rice stalk dust: A mechanical study. Mater Today Proc. 2021;47:5966–9.
[26] Bolka S, Slapnik J, Rudolf R, Bobovnik R, Mešl M. Thermal and mechanical properties of biocomposites based on green PE-HD and hemp fibers. Contemp Mater. 2017;8(1):80–90.
[27] Cestari SP, Albitres G, Mendes LC, Altstädt V, Gabriel JB, Avila G, et al. Advanced properties of composites of recycled high-density polyethylene and microfibers of sugarcane bagasse. J Compos Mater. 2018;52(7):867–76.
[28] Mendes JF, Martins JT, Manrich A, Luchesi BR, Dantas A, Vanderlei RM, et al. Thermo-physical and mechanical characteristics of composites based on high-density polyethylene (HDPE) e spent coffee grounds (SCG). J Polym Env. 2021;29(9):2888–900.
[29] García E, Louvier-Hernández JF, Cervantes-Vallejo FJ, Flores-Martínez M, Hernández R, Alcaraz-Caracheo LA, et al. Mechanical, dynamic and tribological characterization of HDPE/peanut shell composites. Polym Test. 2021;98:107075.
[30] Laftah WA, Majid RA, Ibrahim AN. Preparation and characterization of bio-film composite based on high density polyethylene and oil palm trunk fiber. Polym Polym Compos. 2022;30:096739112210959. doi: 10.1177/09673911221095988.
[31] Satapathy S, Kothapalli RVS. Mechanical, dynamic mechanical and thermal properties of banana fiber/recycled high density polyethylene biocomposites filled with flyash cenospheres. J Polym Env. 2018;26(1):200–13.
[32] Li Y, Hu C, Yu Y. Interfacial studies of sisal fiber reinforced high density polyethylene (HDPE) composites. Compos Part A Appl Sci Manuf. 2008;39(4):570–8.
[33] Colom X, Carrasco F, Pagès P, Canavate J. Effects of different treatments on the interface of HDPE/lignocellulosic fiber composites. Compos Sci Technol. 2003;63(2):161–9.
[34] Suárez L, Castellano J, Díaz S, Tcharkhtchi A, Ortega Z. Are natural-based composites sustainable? Polym (Basel). 2021;13(14):2326.
[35] Aziz T, Haq F, Farid A, Kiran M, Faisal S, Ullah A, et al. Challenges associated with cellulose composite material: Facet engineering and prospective. Env Res. 2023;223:115429.
[36] Ismail H, Ilyas SSM. Recycled polymer blends and composites. Cham: Springer; 2023. doi: 10.1007/978-3-031-37046-5.
[37] Suárez L, Barczewski M, Kosmela P, Marrero MD, Ortega Z. Giant reed (*Arundo donax* L.) fiber extraction and characterization for its use in polymer composites. J Nat Fibers. 2023;20(1):1–14.
[38] Suárez L, Hanna PR, Ortega Z, Barczewski M, Kosmela P, Millar B, et al. Influence of giant reed (*Arundo donax* L.) culms processing procedure on physicochemical, rheological, and thermomechanical properties of polyethylene composites. J Nat Fibers. 2024;21(1). doi: 10.1080/15440478.2023.2296909.
[39] Suárez L, Castellano J, Romero F, Marrero MD, Benítez AN, Ortega Z. Environmental hazards of giant reed (*Arundo donax* l.) in the macaronesia region and its characterisation as a potential source for the production of natural fibre composites. Polym (Basel). 2021;13(13). doi: 10.3390/polym13132101.
[40] Suárez L, Billham M, Garrett G, Cunningham E, Marrero MD, Ortega Z. A new image analysis assisted semi-automatic geometrical measurement of fibers in thermoplastic composites: a case study on giant reed fibers. J Compos Sci. 2023;7(8):326.
[41] Suárez L, Billham M, Garrett G, Cunningham E, Marrero MD, Ortega Z. A new approach for semi-automatic measurement and morphological analysis of fibres throughout thermoplastic compounding process: a case study on giant reed fibers. In 6th International Conference on Natural Fibers 2023. Nature Inspired Sustainable Solutions; 2023. p. 100–2.
[42] Suárez L, Ní Mhuirí A, Millar B, McCourt M, Cunningham E, Ortega Z. Recyclability assessment of lignocellulosic fiber composites: reprocessing of giant reed/HDPE composites by compression molding. In: Hamrol A, Grabowska M, Hinz M, editors. Manufacturing 2024. Cham: Springer; 2024. p. 198–212. doi: 10.1007/978-3-031-56474-1_15.
[43] Tarani E, Arvanitidis I, Christofilos D, Bikiaris DN, Chrissafis K, Vourlias G. Calculation of the degree of crystallinity of HDPE/GNPs nanocomposites by using various experimental techniques: a comparative study. J Mater Sci. 2023;58(4):1621–39.
[44] Prociak A, Sterzyński T, Pielichowski J. Thermal diffusivity of polyurethane foams measured by the modified Angstrom method. Polym Eng Sci. 1999;39(9):1689–95.
[45] Jakubowska P, Sterzyński T. Thermal diffusivity of polyolefin composites highly filled with calcium carbonate. Polimery. 2012;57(4):271–5.
[46] Brostow W, Hagg Lobland HE, Khoja S. Brittleness and toughness of polymers and other materials. Mater Lett. 2015;159:478–80.
[47] Kubát J, Rigdahl M, Welander M. Characterization of interfacial interactions in high density polyethylene filled with glass spheres using dynamic-mechanical analysis. J Appl Polym Sci. 1990;39(7):1527–39.
[48] Podara C, Termine S, Modestou M, Semitekolos D, Tsirogiannis C, Karamitrou M, et al. Recent trends of recycling and upcycling of polymers and composites: a comprehensive review. Recycling. 2024;9(3):37.
[49] Fonseca-Valero C, Ochoa-Mendoza A, Arranz-Andrés J, González-Sánchez C. Mechanical recycling and composition effects on the properties and structure of hardwood cellulose-reinforced high density polyethylene eco-composites. Compos Part A Appl Sci Manuf. 2015;69:94–104.
[50] Bhattacharjee S, Bajwa DS. Degradation in the mechanical and thermo-mechanical properties of natural fiber filled polymer composites due to recycling. Constr Build Mater. 2018;172:1–9.
[51] Spicker C, Rudolph N, Kühnert I, Aumnate C. The use of rheological behavior to monitor the processing and service life properties of recycled polypropylene. Food Packag Shelf Life. 2019;19:174–83.
[52] Barbeş L, Rădulescu C, Stihi C. ATR-FTIR spectrometry characterisation of polymeric materials. Rom Rep Phys. 2014;66(3):765–77.

[53] Huang PW, Peng HS. Number of times recycled and its effect on the recyclability, fluidity and tensile properties of polypropylene injection molded parts. Sustainability. 2021;13(19):11085.
[54] Yin S, Tuladhar R, Shi F, Shanks RA, Combe M, Collister T. Mechanical reprocessing of polyolefin waste: A review. Polym Eng Sci. 2015;55(12):2899–909.
[55] González-Sánchez C, Fonseca-Valero C, Ochoa-Mendoza A, Garriga-Meco A, Rodríguez-Hurtado E. Rheological behavior of original and recycled cellulose-polyolefin composite materials. Compos Part A Appl Sci Manuf. 2011;42(9):1075–83.
[56] Correa-Aguirre JP, Luna-Vera F, Caicedo C, Vera-Mondragón B, Hidalgo-Salazar MA. The effects of reprocessing and fiber treatments on the properties of polypropylene-sugarcane bagasse biocomposites. Polym (Basel). 2020;12(7). doi: 10.3390/POLYM12071440.
[57] Benoit N, González-Núñez R, Rodrigue D. Long-term closed-loop recycling of high-density polyethylene/flax composites. Prog Rubber, Plast Recycl Technol. 2018;34(4):171–99.
[58] Thomasset J, Carreau PJ, Sanschagrin B, Ausias G. Rheological properties of long glass fiber filled polypropylene. J Nonnewton Fluid Mech. 2005;125(1):25–34.
[59] Le Moigne N, Van Den Oever M, Budtova T. Dynamic and capillary shear rheology of natural fiber-reinforced composites. Polym Eng Sci. 2013;53(12):2582–93.
[60] Barczewski M, Ortega Z, Piaskowski P, Aniśko J, Kosmela P, Szulc J. A case study on the rotomolding behavior of black tea waste and bio-based high-density polyethylene composites: Do active compounds in the filler degrade during processing? Compos Part C Open Access. 2024;13:100437.
[61] Cestari SP, Mendes LC, Altstädt V, Lopes LMA. Upcycling polymers and natural fibers waste – properties of a potential building material. Recycling. 2016;1(1):205–18.
[62] Jubinville D, Chen G, Mekonnen TH. Simulated thermo-mechanical recycling of high-density polyethylene for the fabrication of hemp hurd plastic composites. Polym Degrad Stab. 2023;211:110342.
[63] Chen J, Yan N. Crystallization behavior of organo-nanoclay treated and untreated kraft fiber-HDPE composites. Compos Part B Eng. 2013;54(1):180–7.
[64] Dorigato A. Recycling of polymer blends. Adv Ind Eng Polym Res. 2021;4(2):53–69.
[65] Hejna A, Barczewski M, Kosmela P, Aniśko J, Szulc J, Skórczewska K, et al. More than just a beer – Brewers' spent grain, spent hops, and spent yeast as potential functional fillers for polymer composites. Waste Manag. 2024;180:23–35.
[66] Song W, Yang Y, Cheng X, Jiang M, Zhang R, Militky J, et al. Utilization of spent coffee grounds as fillers to prepare polypropylene composites for food packaging applications. Microsc Res Tech. 2023;86(11):1475–83.
[67] Barczewski M, Suárez L, Mietliński P, Kloziński A, Ortega Z. Relationship between the shape of giant reed-based fillers and thermal properties of polyethylene composites: structural related thermal expansion and diffusivity studies. Waste Biomass Valoriz. 2024;15:1–10.
[68] Mendes AA, Cunha AM, Bernardo CA. Study of the degradation mechanisms of polyethylene during reprocessing. Polym Degrad Stab. 2011;96(6):1125–33.
[69] Lu JZ, Wu Q, Negulescu II, Chen Y. The influences of fiber feature and polymer melt index on mechanical properties of sugarcane fiber/polymer composites. J Appl Polym Sci. 2006;102(6):5607–19.
[70] Stanciu MD, Draghicescu HT, Tamas F, Terciu OM. Mechanical and rheological behaviour of composites reinforced with natural fibres. Polymers. 2020;12(6):1402.
[71] Molefi JA, Luyt AS, Krupa I. Comparison of the influence of copper micro- and nano-particles on the mechanical properties of polyethylene/copper composites. J Mater Sci. 2010;45(1):82–8.
[72] Barczewski M, Matykiewicz D, Mysiukiewicz O, MacIejewski P. Evaluation of polypropylene hybrid composites containing glass fiber and basalt powder. J Polym Eng. 2018;38(3):281–9.
[73] Lozano-Sánchez LM, Bagudanch I, Sustaita AO, Iturbe-Ek J, Elizalde LE, Garcia-Romeu ML, et al. Single-point incremental forming of two biocompatible polymers: an insight into their thermal and structural properties. Polym (Basel). 2018;10(4):391.
[74] Ramzy A. Recycling aspects of natural fibre reinforced polypropylene composites. Clausthal: Clausthal University of Technology; 2018.
[75] de Carvalho MS, Azevedo JB, Barbosa JDV. Effect of the melt flow index of an HDPE matrix on the properties of composites with wood particles. Polym Test. 2020;90:106678.
[76] Jyoti J, Singh BP, Arya AK, Dhakate SR. Dynamic mechanical properties of multiwall carbon nanotube reinforced ABS composites and their correlation with entanglement density, adhesion, reinforcement and C factor. RSC Adv. 2016;6(5):3997–4006.
[77] Liu Y, Li H, Ji Z, Kashimura Y, Tang Q, Furukawa K, et al. Molecular structure, crystallinity and morphology of polyethylene/polypropylene blends studied by raman mapping, scanning electron microscopy, wide angle X-ray diffraction, and differential scanning calorimetry. Polym J. 2006;38(11):1127–36.
[78] Wu X, Pu L, Xu Y, Shi J, Liu X, Zhong Z, et al. Deformation of high density polyethylene by dynamic equal-channel-angular pressing. RSC Adv. 2018;8(40):22583–91.
[79] Wang C, Bai S, Yue X, Long B, Choo-Smith LP. Relationship between chemical composition, crystallinity, orientation and tensile strength of kenaf fiber. Fibers Polym. 2016;17(11):1757–64.
[80] Barreto ACH, Esmeraldo MA, Rosa DS, Fechine PBA, Mazzetto SE. Cardanol biocomposites reinforced with jute fiber: Microstructure, biodegradability, and mechanical properties. Polym Compos. 2010;31(11):1928–37.
[81] Sewda K, Maiti SN. Crystallization and melting behavior of HDPE in HDPE/teak wood flour composites and their correlation with mechanical properties. J Appl Polym Sci. 2010;118(4):2264–75.
[82] Li J, Yang S, Turng LS, Zheng W, Jiang S. Comparative study of crystallization and lamellae orientation of isotactic polypropylene by rapid heat cycle molding and conventional injection molding. E-Polymers. 2017;17(1):71–81.
[83] Lila MK, Singhal A, Banwait SS, Singh I. A recyclability study of bagasse fiber reinforced polypropylene composites. Polym Degrad Stab. 2018;152:272–9.
[84] Åkesson D, Fuchs T, Stöss M, Root A, Stenvall E, Skrifvars M. Recycling of wood fiber-reinforced HDPE by multiple reprocessing. J Appl Polym Sci. 2016;133(35):43877.
[85] Shahi P, Behravesh AH, Daryabari SY, Lotfi M. Experimental investigation on reprocessing of extruded wood flour/HDPE composites. Polym Compos. 2012;33(5):753–63.
[86] González-Aguilar SE, Robledo-Ortíz JR, Arellano M, Martín del Campo AS, Rodrigue D, Pérez-Fonseca AA. Mechanical recycling of biobased polyethylene-agave fiber composites. J Thermoplast Compos Mater. 2024;2024:1–21.
[87] Burgstaller C, Renner K. Recycling of wood–plastic composites – a reprocessing study. Macromol. 2023;3(4):754–65.